An Analysis of Forces and Conditions Which Influence the Successful Passage of a Carriage over an Intermediate Support Jack During Downhill Multi-Span Logging

Thomas J. Bobbe

A Paper
Submitted to
School of Forestry
Oregon State University

in partial fulfillment of
the requirements for the
degree of

MASTER OF FORESTRY

Table of Contents

	Page
Abstract	iii
List of Figures	iv
List of Tables	v
Legend of Symbols	vi
I. Introduction	1
II. Literature Review	7
III. Study Objectives	10
IV. Analysis Development	11
Catenary Analysis of Cable Segments	11
Static Force Analysis	14
V. Field Tests	20
Description	20
Test Sequence	21
Field Analysis Results	24
VI. Synthesis of the Catenary Static Force Analysis and Field Test Results	33
Passage onto the Support Jack	33
Passage off of the Support Jack	36
Critical Run Results	42
VII. Discussion	45
VIII. Conclusions and Recommendations for Future Research	52
List of References	54
Appendix 1: Equipment Specifications	56
Appendix 2: HP 41-C Computer Program Listing	59

ABSTRACT

In this paper, a catenary analysis of static skyline, mainline and haulback cable tensions just prior to an unsuccessful attempt by a carriage to pass an intermediate support jack is presented. Field tests were conducted for a range of skyline deflections and span chord slopes. Data collected during the field tests included static and dynamic cable tensions and cable geometry. The relationship between upper span skyline deflection, the percent change in span chord slopes, and their influence on successful carriage passage was determined. During the field tests it was observed that maintaining a taut haulback as the carriage passed the support jack prevented the carriage from surging out of control and reduced dynamic tension fluctuations. It was also observed that yarding the loaded carriage uphill over the support jack was prohibited by skyline deflections which still allowed successful carriage passage for the downhill yarding configuration.

List of Figures

Figures		Page
1	Downhill Multi-span Yarding Configuration.....	5
2	Typical Intermediate Support and Multi-span Equipment.....	6
3a & b	Catenary Cable Segment.....	13
4	Free Body Diagram.....	15
5	The Relationship between the Angles θ, ρ, δ, Tensions ML T_2, SL T_1 and HB T_1	17
6	Skyline Slippage Over the Support Jack Shoe.....	23
7	Geometry of Critical Run.....	25
8a	Static Cable Tensions vs. Skyline Deflection Test A.....	27
8b	Static Cable Tensions vs. Skyline Deflection Test B.....	28
8c	Static Cable Tension vs. Skyline Deflection Test C.....	29
9	A Comparison between Critical Run Static & Dynamic Cable Tensions Just Prior to Passing the Support Jack.....	30
10a & b	Dynamic Cable Tensions Recorded During Critical Runs.....	31, 32
11	Haulback Cable Segment.....	37
12	Computer Program Flow Chart.....	43
13	The Carriage Approaching the Support Jack During a Critical Run.....	48
14	Upper Span Skyline Deflection for Critical Runs vs. Percent Change of Span Chord Slopes for Tests A, B, & C.....	51

LIST OF TABLES

Table		Page
1	Critical Run Dimensions.....	25
2	Static Cable Tensions for Mainline (ML), Haulback (HB) and Skyline (SL) Just Prior to Passing Onto the Support Jack.....	26
3	A Comparison Between the Theoretical and Measured Values for the Critical Run Angle θ of the Skyline Segment.....	42
4	Comparison of Calculated and Measured Static Cable Tensions for Critical Runs.....	44

LIST OF SYMBOLS

α - The direction at which the catenary tension acts.

β - The angle between the vertical distance c and chord segment L for the haulback cable segment (Figure 11).

c - The vertical distance between the haulback chord and cable measured at midspan (Figure 11).

c' - The approximation of the vertical distance described above.

d - The horizontal span between cable segment supports.

δ - The angle between the mainline where it attaches to the carraige and the skyline segment between the carriage and the support jack (Figure 5).

e - The lever arm distance from x_1 at the lower support to the cable weight resultant R.

ε - The direction at which the upper mainline tension acts.

γ - The angle between the haulback chord and the x-axis (Figure 11).

h - The vertical distance between the cable segment supports.

H - The horizontal component of cable tension.

HB T_1 - The haulback lower end tension.

HB T_2 - The haulback upper end tension.

HB H - The horizontal component of the haulback tension.

HB V_1 - The vertical component of the haulback lower end tension.

HB m - The haulback catenary parameter.

HB s - The length of the haulback cable segment.

§ - The upper span chord slope percent (Figure 7).

λ & Ψ - The angles between the skyline cable segments wrapped over the support jack shoe (Figure 6).

L - One half of the haulback chord length (Figure 11).

m - The catenary parameter of a cable segment.

ML T_2 - The mainline upper end tension.

ML H - The horizontal component of the mainline tension.

ML V_2 - The vertical component of the mainline upper end tension.

ML m - The mainline catenary parameter.

ML s - The length of the mainline cable segment.

ϕ - The approximate direction at which tension HB T_2 acts (Figure 11).

R - The resultant force due to cable weight.

ρ - The direction at which tension HB T_1 acts (Figure 5).

S_o - The length of a cable segment

s - The length of a cable segment - general case.

$s_1 + s_2$ - The approximate length of the haulback (Figure 11).

σ - The direction at which tension HB T_2 acts (Figure 11).

SL T_1 - The skyline lower end tension.

SL H - The horizontal component of the skyline tension.

SL V_1 - The vertical component of the skyline lower end tension.

SL m - The skyline catenary parameter.

SL s - The length of the skyline cable segment.

T - The local tension of a cable segment.

T_1 - The lower tension of a cable segment.

T_2 - The upper tension of a cable segment.

θ - The angle of the skyline segment between the support jack and the carriage.

V_1 - The vertical component of lower end cable tension.

V_2 - The vertical component of upper end cable tension.

w - The unit weight of a cable segment.

Wg - The weight of the carriage and payload.

Wg'- The approximate weight of the carriage and payload.

§ - The percent change of the span chord slopes (Figure 7).

x - The x-axis Cartesian coordinate.

y - The y-axis Cartesian coordinate.

ζ - The lower span chord slope percent (Figure 7)

An Analysis of Forces and Conditions which Influence the Successful Passage of a Carriage over an Intermediate Support Jack during Downhill Multi-Span Logging

CHAPTER I

INTRODUCTION

Multi-span logging has become increasingly popular in the Pacific Northwest as a means to access timber beyond the reach of conventional logging systems. In many cases, multi-span logging is economically competitive with conventional logging systems; it offsets the high cost of building frequently spaced roads on steep, difficult terrain by increasing yarding distance.

An integral part of multi-span design is an intermediate support which raises the skyline off the ground and creates two separate spans each with payload capability greater than the single span they replaced. It is possible, though not common, to use more than one intermediate support to yard difficult terrain with convex slopes.

Multi-span logging originated in Europe and was introduced to this country during the 1950's. European multi-span logging can be classified as two general types (McGonagill 1978): 1) gravity systems which lower the turn of logs over the spans to the landing with the yarder usually located at the top of the setting, and 2) endless line systems which allow the yarder to be placed anywhere

along the profile. The turn of logs can be yarded either uphill or downhill.

The gravity system is the least complicated and was the first multi-span configuration used in this country. Gravity systems are comprised of a fixed skyline and a snubbing line to control the gravity descent of the turn. Full suspension of the turn of logs is required. The yarder, typically a Wyssen or Baco single drum, sled mounted machine, has the capabilities to winch itself into yarding position, thus eliminating the need to have road access to the top of the setting.

The multi-span configuration most commonly used in this country is a variation of the gravity system adapted to yard uphill to a landing where the yarder is located. The uphill yarding configuration also requires two lines: a skyline and a mainline. Partial suspension of the turn of logs is a yarding option since the mainline provides power during the inhaul portion of the yarding cycle. The unloaded carriage returns for the next turn under the influence of gravity during the outhaul portion of the yarding cycle. A third line, a haulback, can be used to facilitate carriage outhaul when yarding terrain with moderate slopes.

Recently, a variation of the endless line systems has been proposed to yard downhill where road access to the top of the setting is not feasible or practical. This configuration as shown on Figure 1 replaces the endless line, which controls carriage and lateral inhaul-outhaul, with a mainline and haulback. Replacing the endless

line with two separate lines eliminates the difficulties associated with having to splice the endless line for each new setting and maintaining proper line tension during yarding.

This configuration also has the following advantages over the gravity system: 1) conventional yarders can be used, 2) yarder fueling and maintenance is easier, and 3) the turn of logs can be partially suspended since the mainline provides power for the inhaul.

Probably the most challenging aspect of multi-span logging is the location and design of the intermediate supports. There are a variety of ways in which an intermediate support can be rigged. A schematic drawing of an intermediate support commonly used in the Pacific Northwest is shown in Figure 2.

There has been a reluctance on the part of some loggers to try multi-span logging because they perceive the rigging of an intermediate support as a costly, time consuming operation. Multi-span logging does require more rigging time than a single span skyline operation. However, these additional costs should be viewed in light of the savings associated with not having to build a road to areas inaccessible to single span skyline yarding. In addition, an intermediate support can increase the payload capability of a marginal single span skyline operation and thus increase yarding productivity.

The actual passage of the loaded carriage over an intermediate support jack also influences yarding productivity. Smooth passage of the loaded carriage over the support jack contributes to efficient

multi-span yarding. This paper will examine some of the conditions and analyze the forces required for successful carriage passage over an intermediate support jack for the downhill yarding configuration shown in Figure 1.

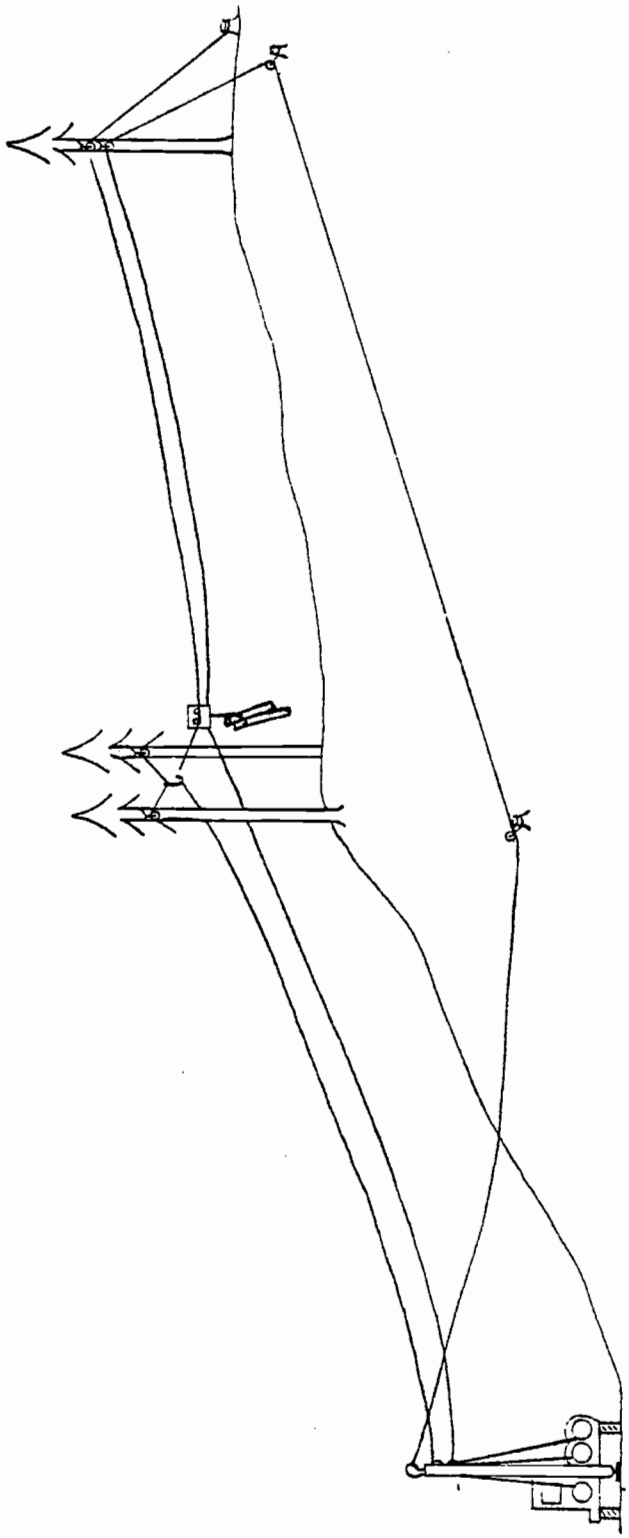

Figure 1. Downhill Multi-span Yarding Configuration

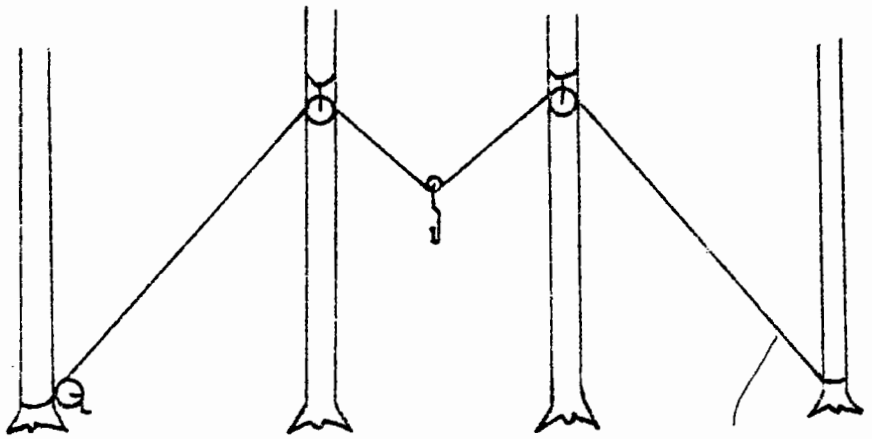

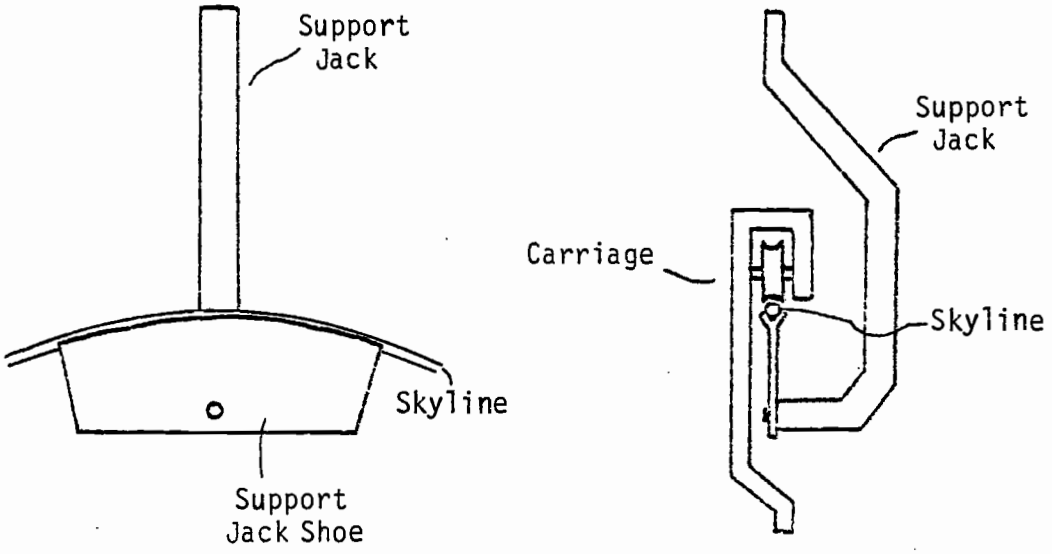

Figure 2. Typical Intermediate Support and Multi-span Equipment

CHAPTER II

LITERATURE REVIEW

Much of the recent work on multi-span logging has been focused on uphill yarding configurations. An analysis of uphill multi-span logging has been done by Peters and Aulerich (1977), Brantigan (1978), and Fodge (1981).

Peters and Aulerich (1977) did a production study on uphill multi-span logging with a Schield-Bantam T350 yarder. In addition to collecting time study data, skyline and intermediate support line tensions were recorded during the yarding cycle to assess the adequacy of line sizes and the safety of current rigging practices used for two-tree intermediate supports.

Fodge (1981) conducted a detailed analysis of forces created in two-tree intermediate supports during uphill multi-span logging. His analysis was divided into two parts. The first part determined the maximum force exerted upon the support jack. The second part determined the movement and forces created in the two-tree intermediate support by the skyline and the carriage. He determined that the support line sizes required by the Oregon State Safety Code were more than adequate.

Brantigan (1978) studied the critical conditions for carriage passage during uphill multi-span yarding. He determined that the failure of the carriage to pass over the jack was a function of the

following parameters: mainline tension and its direction of pull at the carriage, chord slope of the skyline spans, gross payload, and skyline length or equivalently skyline tension. He determined that failure to pass the jack could either be caused by insufficient mainline tension to advance the carriage past static equilibrium conditions, or critical geometry conditions developing at the jack. An analysis of the critical skyline and mainline tensions was developed and compared to tensions measured during field testing.

Much of the design criteria for downhill multi-span logging is based on field observations. The Logging Systems Guide compiled by McGonagill (1978) describes a condition which can cause the loaded carriage to have difficulty in passing the jack when yarding downhill under the influence of gravity.

> As the carriage approaches the jack, the weight of the carriage and the turn will pull deflection out of adjacent spans and increase deflection in the loaded span. If this results in the carriage being lower in elevation than the jack to be crossed, the carriage may have trouble passing the jack...

Deflection is the vertical distance at midspan between the cable and the chord (the straight line between the cable ends) divided by the horizontal distance of the span. Deflection is expressed as a percentage.

Both the Logging Systems Guide and The Chain and Board Handbook for Skyline Tension and Deflection, prepared by Binkley and Sessions (1977), state that a combination of too great a change in chord slopes between spans and too much skyline deflection will prevent

smooth carriage passage over the jack. They state that a loaded skyline deflection of six percent or less is a good target for designing multi-span layout. In addition, field observations indicate that the change in chord slopes should be less than 35% for uphill yarding and less than 60% for downhill gravity yarding.

There does not appear to be any written guidelines for designing a downhill multi-span configuration as shown in Figure 1.

CHAPTER III

STUDY OBJECTIVES

The general purpose of the study is to determine the cable tensions and geometry necessary for successful passage of the loaded carriage over the support jack during downhill yarding. The specific objectives are:

1) Develop a static analysis of the tension in the skyline, mainline and haulback just prior to an unsuccessful attempt to pass a support jack.
2) In a field test, measure the tensions and geometry of the cable segments of multi-span during carriage passage over a support jack for a range of skyline deflections and chord slopes.
3) Compare the tensions determined in the static analysis to the tensions measured in the field just prior to the unsuccessful attempt to pass a support jack.
4) Determine the relationship between successful carriage passage, upper span loaded skyline deflection and the percent change in span chord slopes.

CHAPTER IV

ANALYSIS DEVELOPMENT

Catenary Analysis of Cable Segments

The analysis of forces in cable segments invariably requires an assumption about the shape of the cable segment. A uniform, flexible cable suspended between two points hanging under the influence of its own weight assumes the shape of a catenary. The derivation of catenary equations involves the relationship between cable segment variables and hyperbolic sine and cosine functions (Carson 1977).

Catenary equations most accurately describe the forces and shape of cable segments through the range of taut and slack conditions. However, the catenary analysis of cables in a logging systems problem often requires an iterative solution since certain key variables are not known and can not be solved for directly.

Another solution technique for cable segments, the Rigid Link approximation, determines the cable tensions directly, but is inaccurate for slack conditions.

The catenary equations of cable segments shown in Figure 3a and 3b are described by Carson (1977). The following equations apply to the cable segment shown in Figure 3a:

$$y = m \cosh (x/m) \qquad \text{eq. 1}$$

$$x = m \cosh^{-1} (y/m) \qquad \text{eq. 2}$$

$$S_o = m \sinh (x/m) \qquad \text{eq. 3}$$

$$T = w\, m \cosh (x/m) \qquad \text{eq. 4}$$

$$V = w\, m \sinh (x/m) \qquad \text{eq. 5}$$

$$m = H/w \qquad \text{eq. 6}$$

where:

w = the unit weight of the cable segment

m = the catenary parameter for the segment

y = the y-axis Cartesian coordinate

x = the x-axis Cartesian coordinate

S_o = the length of the cable segment

T = the local tension of the cable segment

V = the vertical component of the tension

H = the horizontal component of the tension

α = the direction at which the tension acts

For the general case cable segment shown in Figure 3b, the following equations apply:

$$T_2 = (w/2) (s \coth (d/2m) + h) \qquad \text{eq. 7}$$

$$V_2 = (w/2) (h \coth (d/2m) + s) \qquad \text{eq. 8}$$

$$T_1 = (w/2) (s \coth (d/2m) - h) \qquad \text{eq. 9}$$

or

$$T_1 = T_2 - wh \qquad \text{eq. 10}$$

$$V_1 = (w/2) (h \coth (d/2m) - s) \qquad \text{eq. 11}$$

or

$$V_1 = V_2 - ws \qquad \text{eq. 12}$$

$$s = (h^2 + (2m \sinh (d/2m))^2)^{\frac{1}{2}} \qquad \text{eq. 13}$$

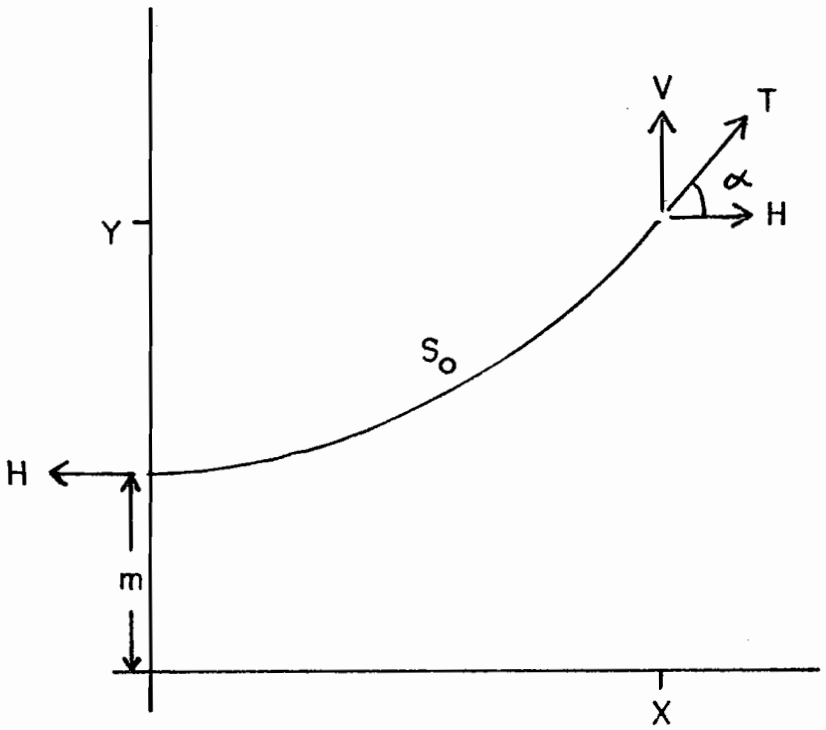

Figure 3a. Catenary Cable Segment.

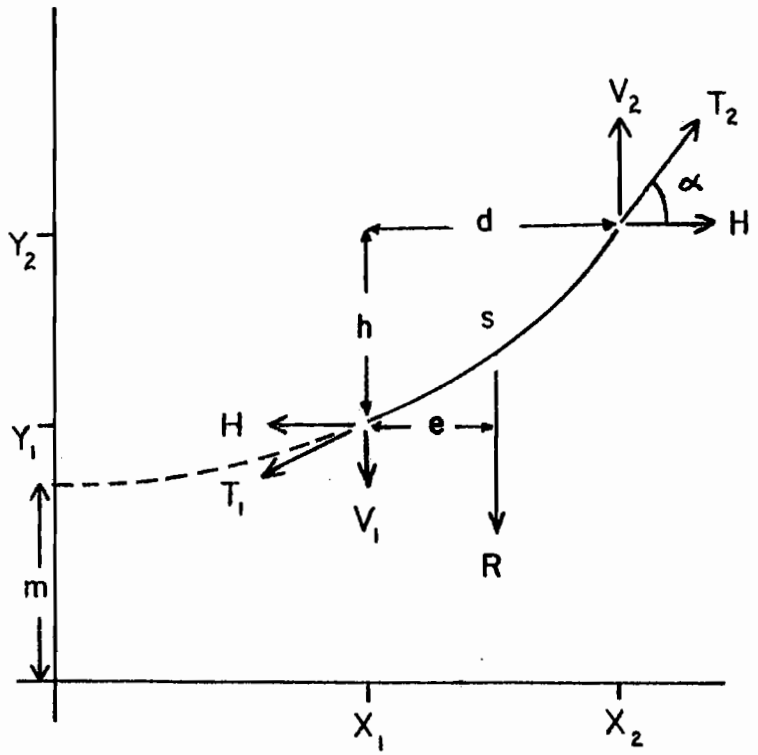

Figure 3b. Catenary Cable Segment - General Case.

$$y_1 = m \cosh (X_1/m) \qquad \text{eq. 14}$$

or

$$y_1 = T_1/w \qquad \text{eq. 15}$$

$$X_1 = m \cosh^{-1} (y_1/m) \qquad \text{eq. 16}$$

where:

s = the length of the cable segment between supports

T_2 = the upper tension of the cable segment

V_2 = the upper vertical component of the tension

T_1 = the lower tension of the cable segment

V_2 = the lower vertical component of the tension

R = the resultant force due to the cable weight

e = the lever arm of the force R from X_1

d = the horizontal span between supports

h = the elevation difference between supports

Static Force Analysis

The static analysis of forces in the skyline, mainline and haulback as the loaded carriage approaches the jack, is accomplished by considering the free body diagram on the following page.

The assumptions of this analysis are:

1) The payload is fully suspended as the carriage approaches the jack.
2) The carriage sheaves riding on the skyline are frictionless.
3) The effect of cable stretch is negligible.

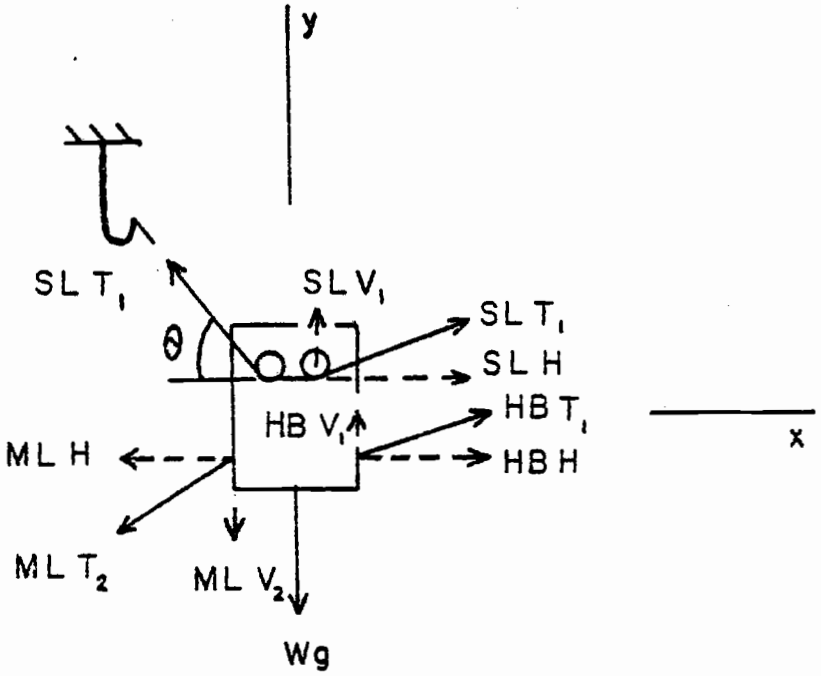

Figure 4. Free Body Diagram.

where:

ML T_2 = the upper mainline tension

ML H = the horizontal component of the mainline tension

ML V_2 = the vertical component of the upper mainline tension

SL T_1 = the lower skyline tension

SL H = the horizontal component of the skyline tension

SL V_1 = the vertical component of the lower skyline tension

HB T_1 = the lower haulback tension

HB H = the horizontal component of the haulback tension

HB V_1 = the vertical component of the lower haulback tension

θ = the angle of the skyline segment between the support jack and the carriage

Wg = the weight of the carriage and payload

By summing the forces, the equations of static equilibrium become:

$$\Sigma Fx: -SL\ T_1 \cos\theta - ML\ H + SL\ H + HB\ H = 0 \qquad \text{eq. 17}$$

$$\Sigma Fy: SL\ T_1 \sin\theta + SL\ V_1 + HB\ V_1 - ML\ V_2 - Wg = 0 \qquad \text{eq. 18}$$

A closer look at the free body diagram reveals the relationship between the angle θ, tensions ML T_2, HB T_1, SL T_1, weight Wg, skyline length and the slope of the spans.

The skyline length has the most obvious effect on the angle θ. For a given upper span chord slope and chord length, the angle θ can be increased by lengthening the skyline until the resultant of forces SL T_1 in the two skyline segments no longer has a negative horizontal component according to the coordinate axis shown in Figure 4. The direction at which this skyline resultant acts can be found by bisecting the angle between the two skyline segments. Steeper slopes in the upper span allow longer skyline lengths and larger values for θ which still result in a negative component. A negative horizontal component is a necessary condition for carriage passage in the gravity inhaul configuration.

This is not a necessary condition for the configuration being studied, since the mainline is able to provide the force necessary to advance the carriage onto the support jack. However, as the angle between ML T_2 and SL T_1 of the skyline segment between the carriage and the support jack approaches 90 degrees, the component of ML T_2

acting in the direction that the carriage has to travel over the skyline, becomes zero. Figure 5 displays this relationship graphically.

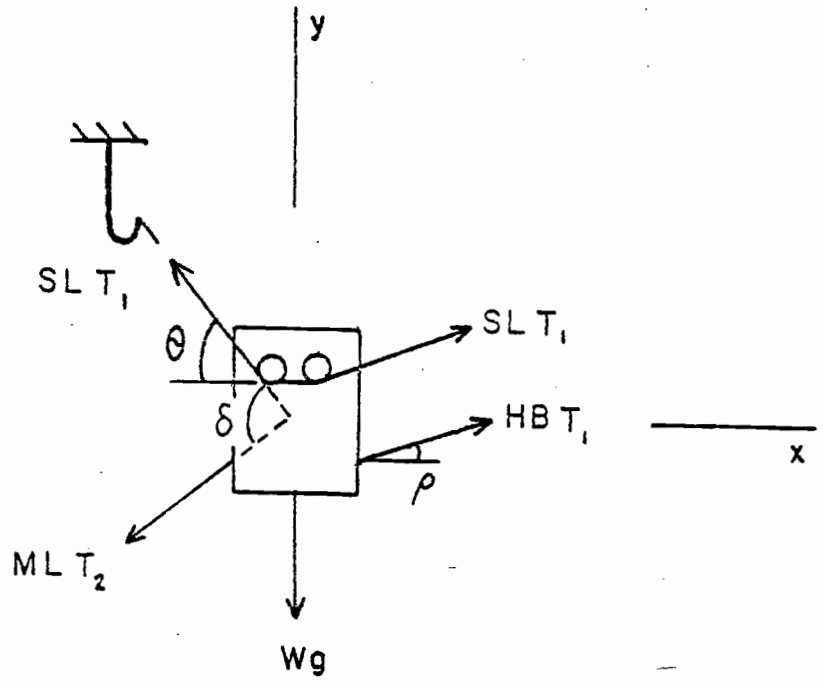

Figure 5. The Relationship Between the Angles θ, ρ, δ, Tensions ML T_2, SL T_1 and HB T_1.

The component of ML T_2 acting in the direction of the skyline segment is a function of MLT_2 cos δ. As δ approaches 90 degrees, the magnitude of ML T_2 must be increased to maintain this force component. Increasing ML T_2 will in turn pull the skyline in the upper span taut and increase the angle θ. Increasing Wg will also contribute to pulling the skyline taut.

The resultant of the skyline forces influences the amount of mainline tension necessary to advance the carriage onto the support jack. While the skyline resultant does not need to have a negative

horizontal component, as the resultant of forces SL T_1 becomes vertical, the magnitude of force ML T_2 required to move the carriage onto the support jack decreases. Increasing the angle of ρ will also increase the vertical component of HB T_1.

As mentioned previously, the angle θ is influenced by the direction at which ML T_2 pulls on the carriage. The direction of ML T_2 is a function of the slope of the lower span and the amount of tension in the mainline. The tension of a taut mainline will be limited by cable strength or yarder power. As the mainline is pulled taut, the direction of ML T_2 approaches the angle which is described by the straight line between the mainline sheave on the tower and the point of attachment on the carriage. Therefore, when the mainline is taut, the angle θ decreases as the slope of the lower span increases.

There are two modes of failure which describe the inability of the carriage to advance onto the support jack:

1) The first mode deals with the geometry of the cable segments shown in Figure 5. If the angle θ is increased to a point where the angle δ is greater than or equal to 90 degrees, the mainline will not be able to pull the carriage onto the support jack.

2) The second mode addresses the upper limit of the mainline tension. Tension ML T_2 will be limited by either the breaking strength of the cable or by the maximum amount of line pull that the yarder can provide.

Inspection of the free body diagram also reveals that the forces on the carriage are statically indeterminant due to a redundant con-

straint. There are more constraints than necessary to ensure a stable position. In this case the haulback is an unknown redundant constraint.

To solve for the forces in the free body diagram prior to an unsuccessful attempt to pass the support jack, the relationship between the failure to pass the support jack and the haulback tension must be known. Field tests of the multi-span configuration were conducted to gather this information.

CHAPTER V

FIELD TESTS

Description

The field tests were conducted on the MacDonald-Dunn Forest. A Christy three-drum small wood yarder equipped with a 5/8" skyline, 9/16" mainline and 7/16" haulback and powered by a 105 hp diesel engine was used for the tests. A concrete block was suspended from a multi-span "truck" which served as a carriage. The combined weight was 1,100 lbs.

Due to a limited amount of time available for use of the yarder, three chord slope arrangements with one gross payload were tested. The three chord slope arrangements were rigged over the same ground profile to reduce set-up and tear-down time. The rigging heights of the support jack and tail-tree were varied to test a range of chord slope combinations.

Ground profile coordinates were determined by using a 100' steel tape, level rod and self-leveling level. The coordinates of the support jack and carriage were determined by using a Theodolite and a 100' steel tape. The elevation of the skyline and haulback rigged in the tail tree was determined by directly measuring the distance from the top of each sheave to a bench mark established on the base of the tail tree. The elevation of the mainline and skyline at the yarder were established in a similar manner.

Load cells were attached to the end of the skyline near the tail tree and at the mainline and haulback connections to the carriage. A combination of three Validyne strain gage amplifiers, one for each load cell, mounted in a Validyne multi-channel module case, measured the changes in electrical resistance of the strain gages mounted on the load cells.

When tension is placed on the load cells, the strain gages are minutely distorted in proportion to the amount of applied tension. This distortion in turn changes the electrical resistance within the strain gage. The change in electrical resistance changes the excitation voltage which is detected by the Validyne strain gage amplifiers. These changes were calibrated and translated to display the applied tension on a Validyne digital panel meter. Static cable tensions were recorded from a digital panel meter while dynamic tensions were recorded on Brush (Gould) strip chart recorders. Complete equipment specifications are listed in Appendix 1.

Test Sequence

Before starting the test runs in each chord slope arrangement, the loaded carriage was yarded over the support jack several times to allow for adjustment of the skyline length. The amount of skyline was increased until carriage passage over the support jack during downhill yarding became noticably difficult.

A test run was then started by positioning the carriage at the upper midspan. A Theodolite stationed near the intermediate support

determined the coordinates of the carriage and support jack by measuring the horizontal and vertical angles to targets marked on each. This information was used to determine the upper midspan deflection. Static tensions in all three load cells were measured by the Validyne unit and recorded.

The carriage was then positioned near the intermediate support at a point on the skyline where the carriage was just about to move onto the support jack. The length of the skyline segment between the carriage and the support jack was less than one foot for all tests. Theodolite measurements were taken on the support jack and carriage targets to provide the information needed to calculate dimensions d and h for the cable segments when the carriage was in the position shown in the free body diagram (Figure 4). Theodolite measurements were also taken on the ends of the skyline segment between the support jack and carriage to determine the angle θ for the critical run. A critical run was defined as one which had a difficult, rough passage. Static tensions in all three load cells were measured and recorded.

The carriage was then returned to the upper midspan position in preparation for the dynamic run over the support jack. The strip chart recorders for the load cells were turned on and the carriage was yarded at normal operating speed over the support jack and stopped at the lower midspan. The carriage was then yarded back to the upper midspan and the skyline length was increased for the next run.

This sequence was repeated until a critical run for downhill yarding was achieved. During each critical run, the carriage had at least one momentary hang-up before passing over the support jack. The skyline would then slip over the support jack shoe, allowing the jack to swing away from the carriage. The carriage would immediately surge after the jack and pass over the support into the next span.

Figure 6 depicts this sequence. During the momentary hang-up, the tension of the skyline in the upper span is greater than the skyline tension in the lower span. As the angle λ decreases, the difference in the skyline tension becomes greater and the frictional force between the skyline and the support jack shoe is overcome. The skyline then slips over the jack, attempting to equalize the skyline tensions in the adjacent spans and the angles λ and ψ.

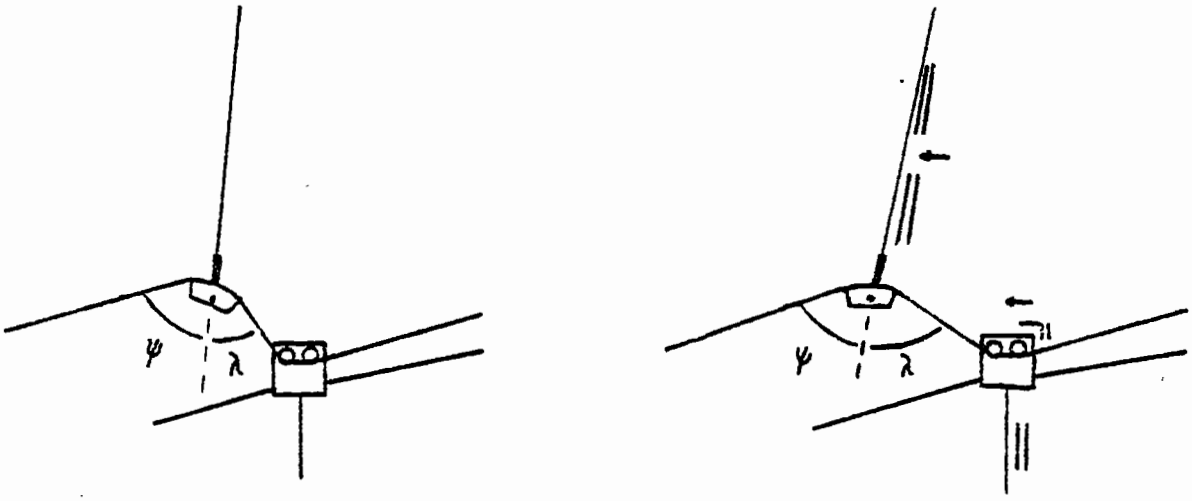

Figure 6. Skyline Slippage Over the Support Jack Shoe

The amount of skyline slippage increased as the deflection of the upper span was increased for each run. An attempt was made to quantify this slippage by painting interval marks on the skyline and filming the support jack as the dynamic run was being made. However, the movie camera used for the filming was not sophisticated enough to capture the rapid movement of the marks under the lighting conditions along the skyline corridor.

During the field tests it was also observed that a rough passage could be caused by inadequate control of the carriage as it left the support jack. When the haulback was not taut enough to snub the carriage as it surged over the jack, the carriage would launch itself into an uncontrolled run down the skyline; particularly during runs with greater breaks in chord slopes. When the haulback was allowed to become too slack, the carriage would run out of control until the slack in the haulback was pulled taut, abruptly stopping the carraige.

Abruptly stopping the carriage would cause increases in dynamic cable tensions. In addition, the mainline would swing about and often wrap itself around the skyline causing a delay in the yarding cycle. To prevent this, the haulback brake on the yarder was used to control the deflection or equivalently the tension.

Field Test Results

The data for the critical run of each of the three chord slope arrangements tested as shown on Figure 7, is listed on Table 1.

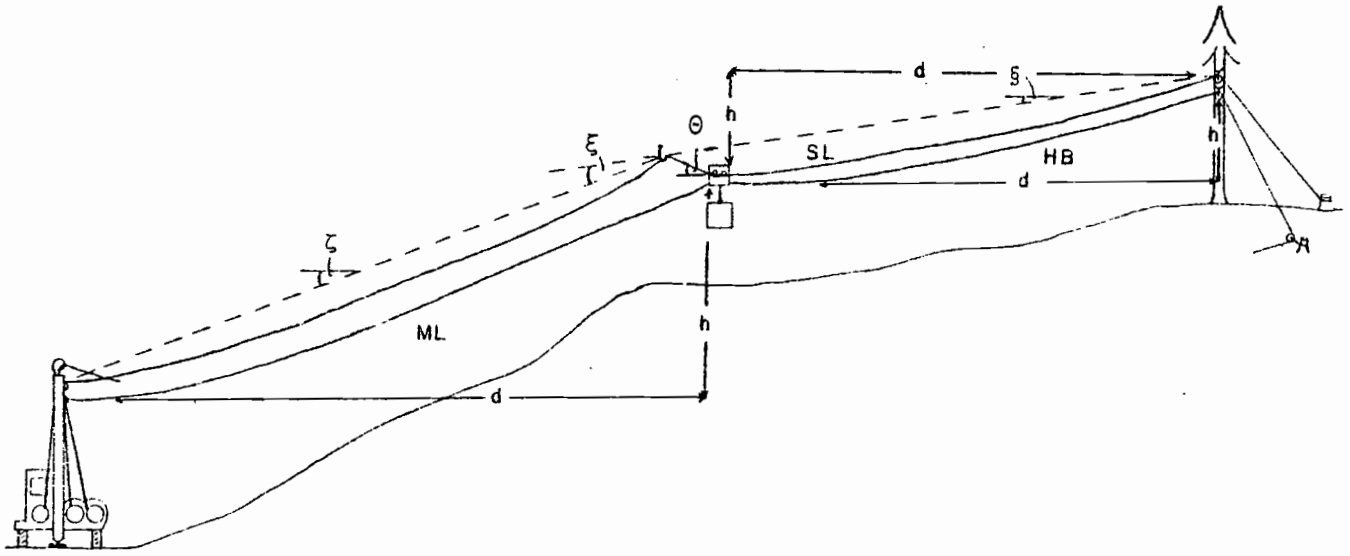

Figure 7. Geometry of Critical Run.

Table 1. Critical Run Cable Dimensions

Test	ζ (%)	§ (%)	ξ(%) [1/]	θ (degrees)	d(ft)	h(ft)
A	42.95	25.69	17.26	52.6	ML 369.25	157.46
					SL 206.15	54.18
					HB 206.15	57.08
B	47.06	18.51	28.55	51.2	ML 368.48	172.17
					SL 206.92	39.47
					HB 206.92	42.37
C	48.89	7.36	41.53	51.8	ML 365.97	177.19
					SL 209.43	16.85
					HB 209.43	20.85

[1/] ξ is the percent change of the span chord slopes.

Table 2 lists the static cable tensions when the carriage was just prior to passing onto the support jack from the upper span. Figures 8a, b and c display these static cable tensions and the upper span skyline deflections for each test run. Figure 9 compares the critical run static and dynamic cable tensions when the carriage was just prior to passing onto the support jack. Figures 10a and b display the dynamic cable tensions recorded during the critical runs for each test.

Table 2. Static Cable Tensions for Mainline (ML), Haulback (HB) and Skyline (SL) Just Prior to Passing onto the Support Jack

Test	Run	ML (lbs)	HB (lbs)	SL (lbs)[1/]
A	1	940	475	3,085
	2	1,005	560	2,690
	3	1,275	540	2,175
	4	1,340	690	1,850
	5	1,480	905	1,795
	6*	1,660	935	1,745
B	1	1,005	420	2,885
	2	1,275	680	2,405
	3	1,360	700	2,240
	4	1,510	720	2,175
	5*	1,910	985	2,005
C	1	1,175	470	2,770
	2	1,320	620	2,525
	3	1,720	680	2,450
	4*	2,175	910	2,480

*critical run

[1/]corrected to read at carriage $T_1 = T_2 - wh$ eq. 10

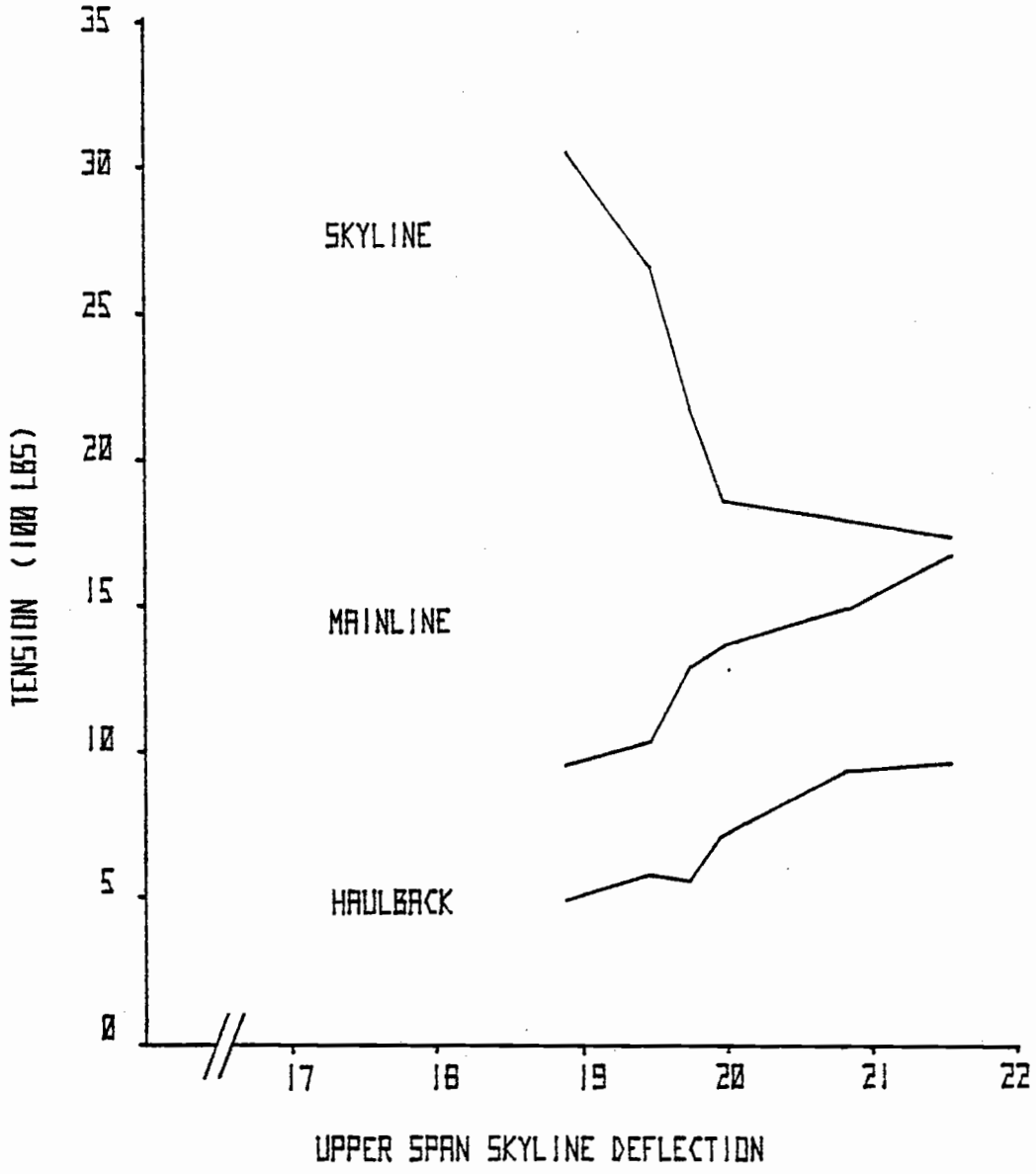

FIGURE 8A. STATIC CABLE TENSIONS VS. SKYLINE DEFLECTION TEST A.

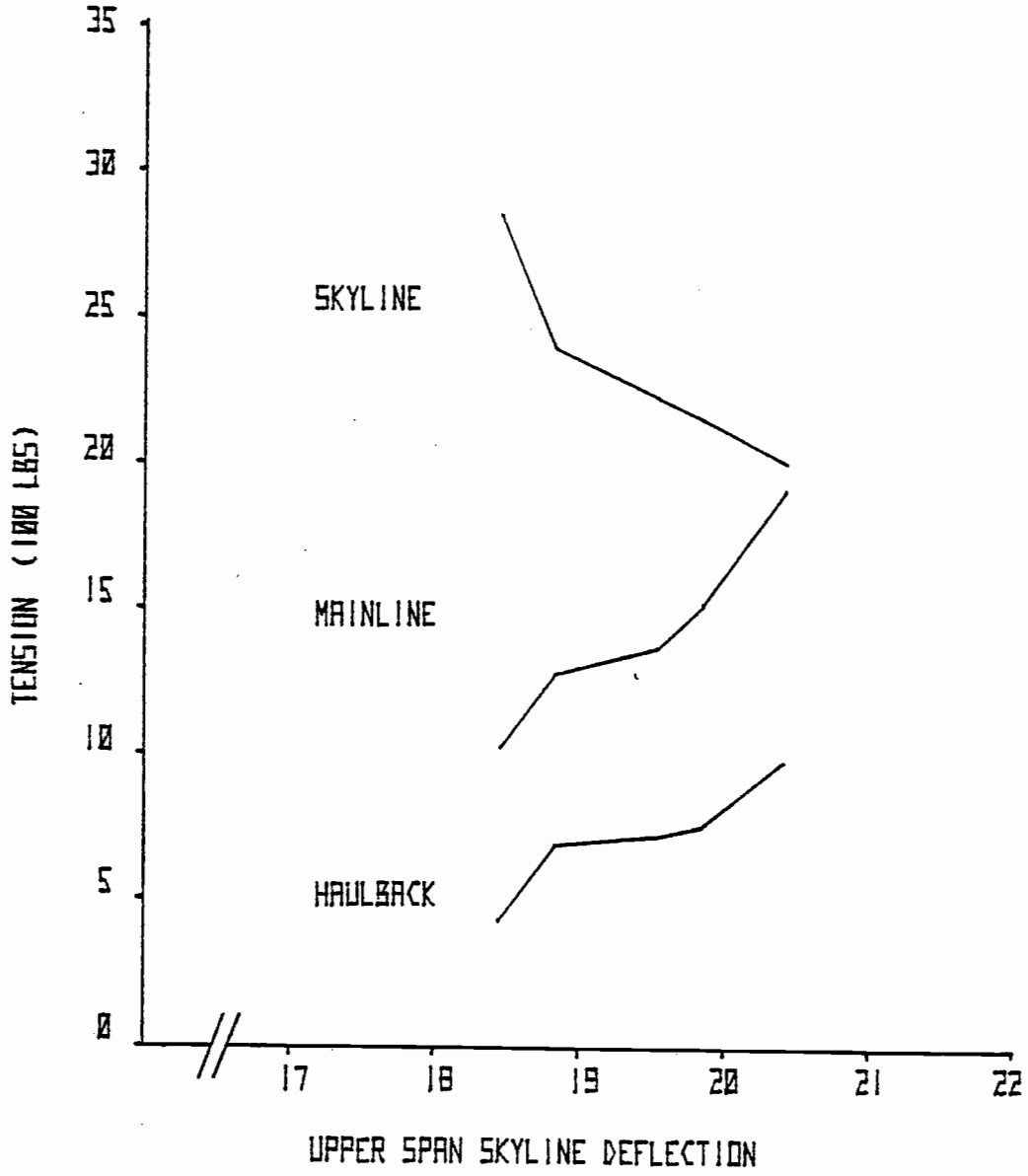

FIGURE 88. STATIC CABLE TENSIONS VS. SKYLINE DEFLECTION TEST B.

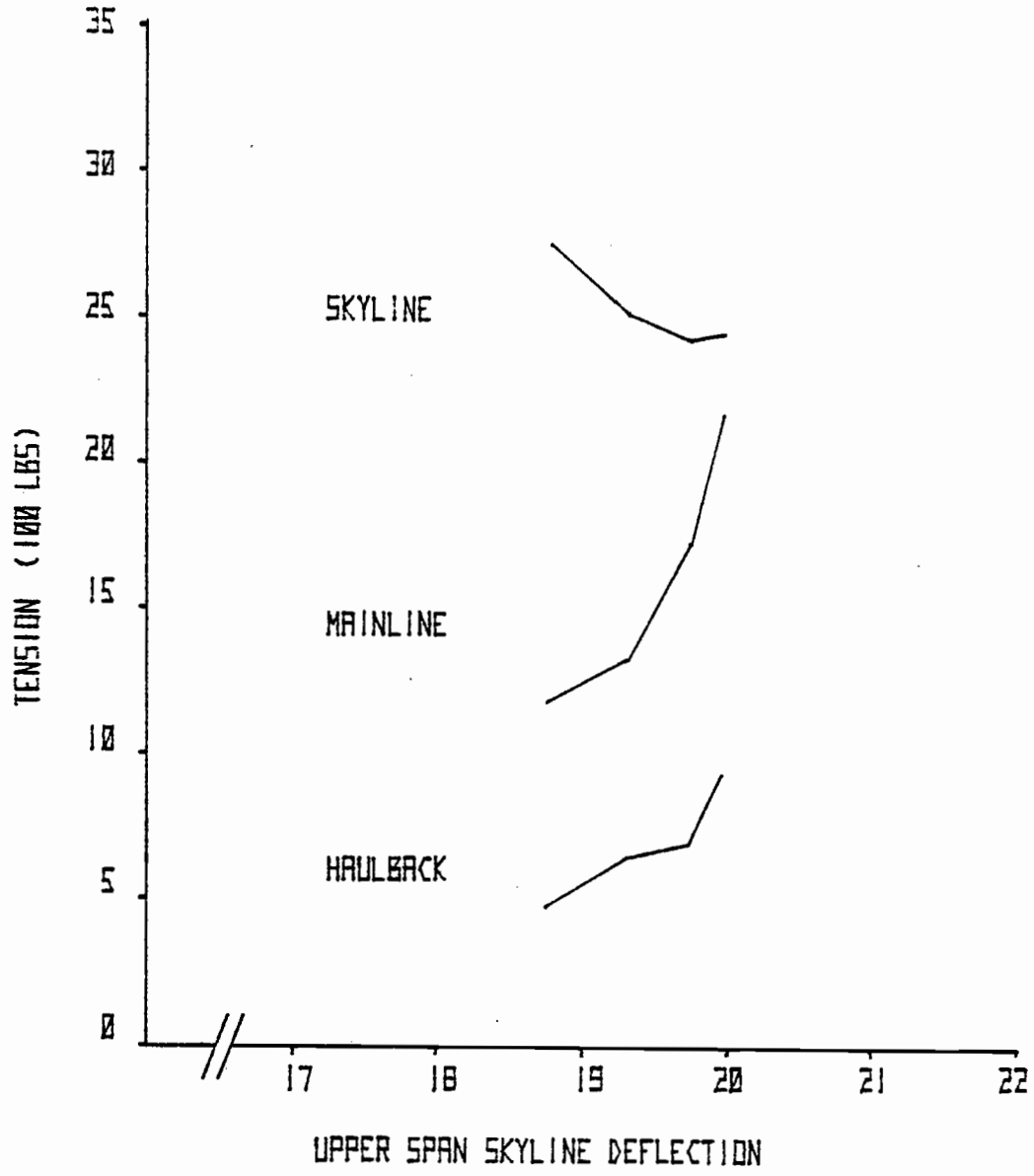

FIGURE 8C. STATIC CABLE TENSIONS VS. SKYLINE DEFLECTION TEST C.

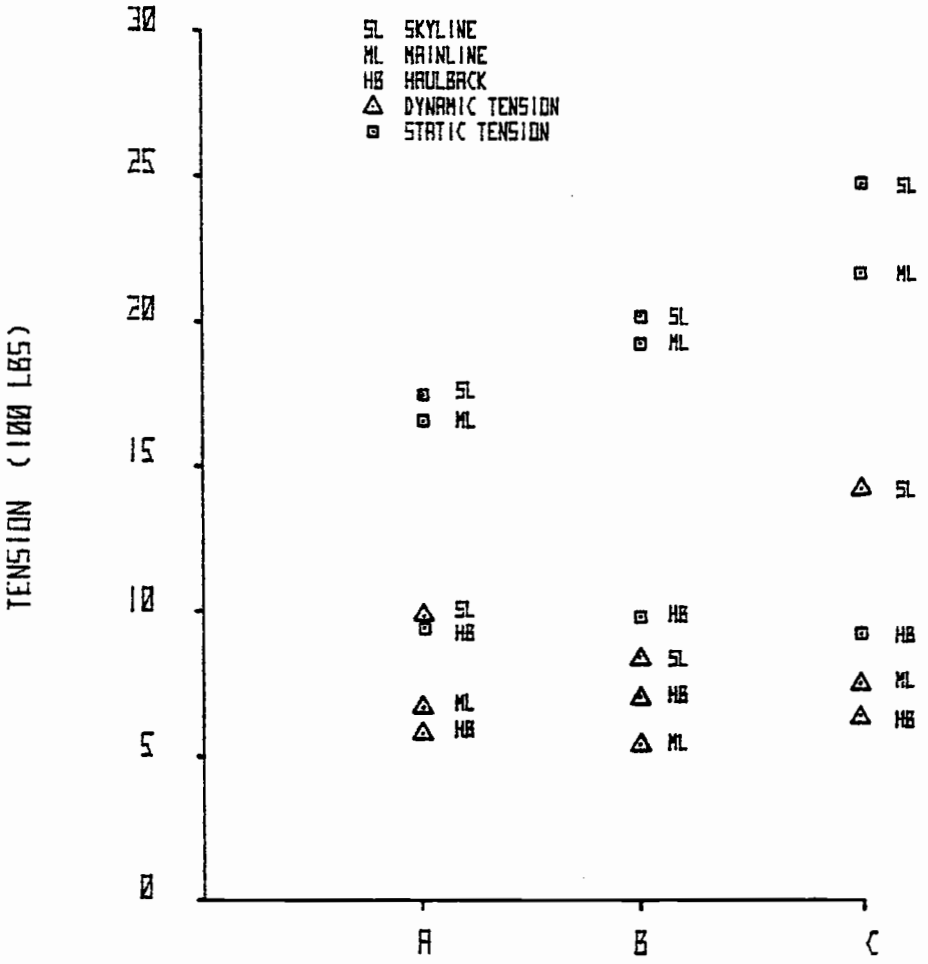

FIGURE 9. A COMPARISON BETWEEN CRITICAL RUN STATIC & DYNAMIC CABLE TENSIONS JUST PRIOR TO PASSING THE SUPPORT JACK.

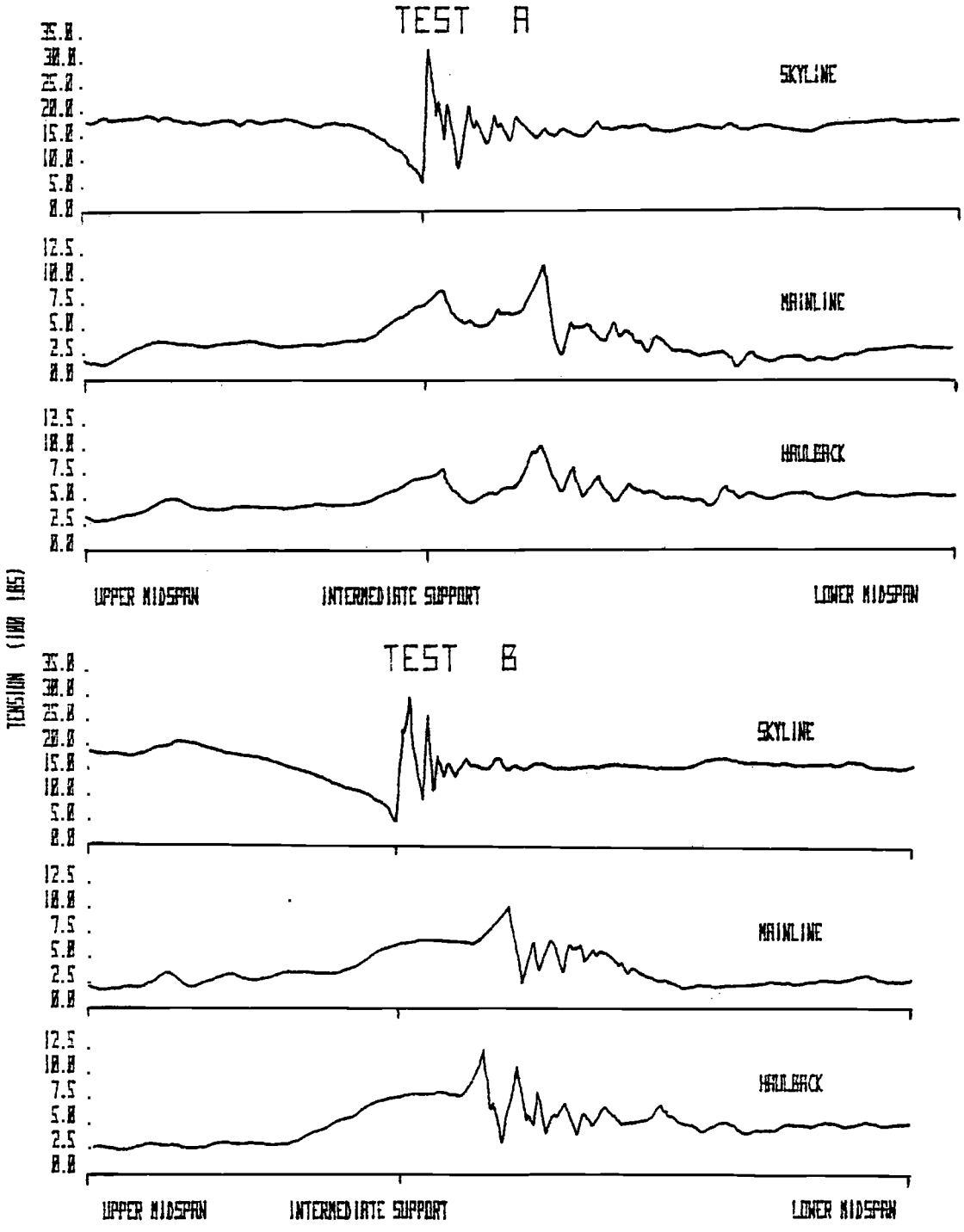

FIGURE 10 A. DYNAMIC CABLE TENSIONS RECORDED DURING CRITICAL RUNS

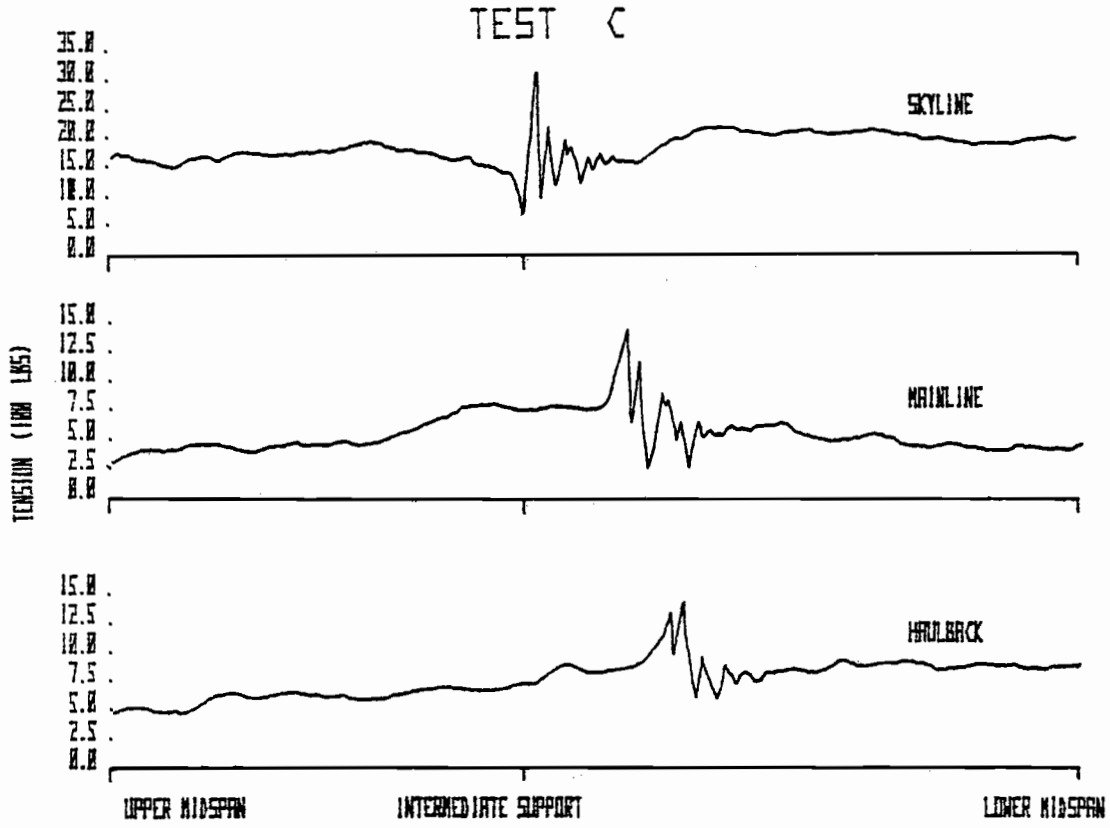

FIGURE 10 B. DYNAMIC CABLE TENSIONS RECORDED DURING CRITICAL RUN

CHAPTER VI

SYNTHESIS OF THE CATENARY STATIC FORCE ANALYSIS AND FIELD TEST RESULTS

Field test results can now be used to complete the catenary static force analysis. A key to the solution of the problem is to recognize that successful carriage passage involves two stages: carriage passage onto and off of the support jack.

Passage onto the support jack

Movement of the carriage onto the support jack is contingent upon the forces and geometry of the cable segments. The direction of mainline tension ML T_2 must be aligned with respect to the geometry of the other cable segments so that it is able to advance the carriage onto the support jack. Since the direction in which ML T_2 acts is a function of its magnitude, an approximation of the maximum mainline tension must be made. As mentioned previously, maximum tension is assumed to be either the breaking strength or, more conservatively, the safe working load of the cable or the maximum mainline drum pull.

The safe working load of the mainline can be obtained from wire rope manufacturer's specifications. The maximum rated mainline drum pull can be obtained from the manufacturer's specifications for the yarder being considered. Since the support jack is higher in elevation than the mainline drum for the downhill yarding configuration,

the tension at the mainline connection to the carriage is calculated by using equation 10: $T_2 = T_1 + wh$. In this case T_1 is the mainline pull at the drum and h is the vertical distance between the point of attachment to the carriage and the yarder drum. The maximum design tension will be the lesser of the cable safe working load or the rated mainline pull at the carriage.

Carson (1977) describes an iterative algorithm which determines the catenary parameters of a cable segment when the tension T_2, d, h and w are known. This approach is based on a moment balance of forces around the anchor point x_1, y_1 of the cable segment shown in Figure 3b.

The following equation is developed:

$$+ \Sigma M_{x_1 y_1} = H\,h + Re - V_2 d = 0 \quad . \qquad \text{eq. 19}$$

Substituting

$$V_2^2 = T_2^2 - H^2 \qquad \text{eq. 20}$$

into equation 19 yields

$$Hh + Re = (T_2^2 - H^2)^{\frac{1}{2}}\, d \quad .$$

This simplifies to

$$(Hh)^2 + 2HR\,he + (Re)^2 - (T_2 d)^2 + (Hd)^2 = 0$$

$$H^2 \left[1 + \left(\frac{h}{d}\right)^2\right] + 2HR\frac{he}{d^2} + R^2 \left(\frac{e}{d}\right)^2 - T_2^2 = 0 \quad . \qquad \text{eq. 21}$$

Using the quadratic formula gives a solution for m,

$$m = \frac{-R(he/d^2) \pm \sqrt{(R(he/d^2))^2 - (1+(h/d)^2)(R^2(e/d)^2 - T_2^2)}}{w\,(1+(h/d)^2)} \quad . \qquad \text{eq. 22}$$

The algorithm starts by making a rigid link approximation for values R and e. The initial approximations are

$$R \doteq w(h^2 + d^2)^{\frac{1}{2}} \qquad \text{eq. 23}$$

and

$$e \doteq d/2 \quad . \qquad \text{eq. 24}$$

These values are substituted into equation 22 to determine the initial value of m. Once m is known, the values of R and e are improved by using the following equations:

$$R = ws = w(h^2+(2m \sinh(d/2m))^2)^{\frac{1}{2}} \qquad \text{eq. 25}$$

and

$$e = d/2 - (h/s)(m-(d/2) \coth (d/2m)) \quad . \qquad \text{eq. 26}$$

These new values of R and e are then substituted back into equation 22 to determine a new value of m. The algorithm continues to cycle through equations 25, 26 and 22 until the improved value of m does not differ appreciably from the previous value. For the calculations used in this study, an allowable tolerance was set at .0001. This algorithm converges on the answer rapidly; usually within three iterations.

The mainline catenary parameter m is determined by using this algorithm. Once the value for m is determined, the horizontal force ML H can be calculated using

$$H = mw \quad . \qquad \text{eq. 6}$$

The angle ε at which tension ML T_2 acts is then found by using

$$\varepsilon = \cos^{-1} (H/ML\ T_2) \quad . \qquad \text{eq. 27}$$

The maximum value for the angle θ of the skyline segment, can be calculated according to

$$\theta = \delta - \varepsilon \qquad \text{eq. 28}$$

where δ, the angle between the skyline segment and the direction of the mainline tension ML T_2 as shown in Figure 5, is equal to 90 degrees.

Passage off of the Support Jack

Movement off of the support jack is controlled by the tension in the haulback. As mentioned previously in the field test chapter, the haulback deflection was controlled by braking the haulback drum as the carriage was yarded in. Too much deflection in the haulback would allow the carriage to surge uncontrolled off of the support jack. Trial and error calculation of the haulback tension determined that using a one percent deflection with the dimensions d and h measured during the field tests yields values which fall within the range of static tensions measured.

Calculation of the haulback tension HB T_2, requires an iterative algorithm when w, d, h and the deflection are known and proceeds as follows:

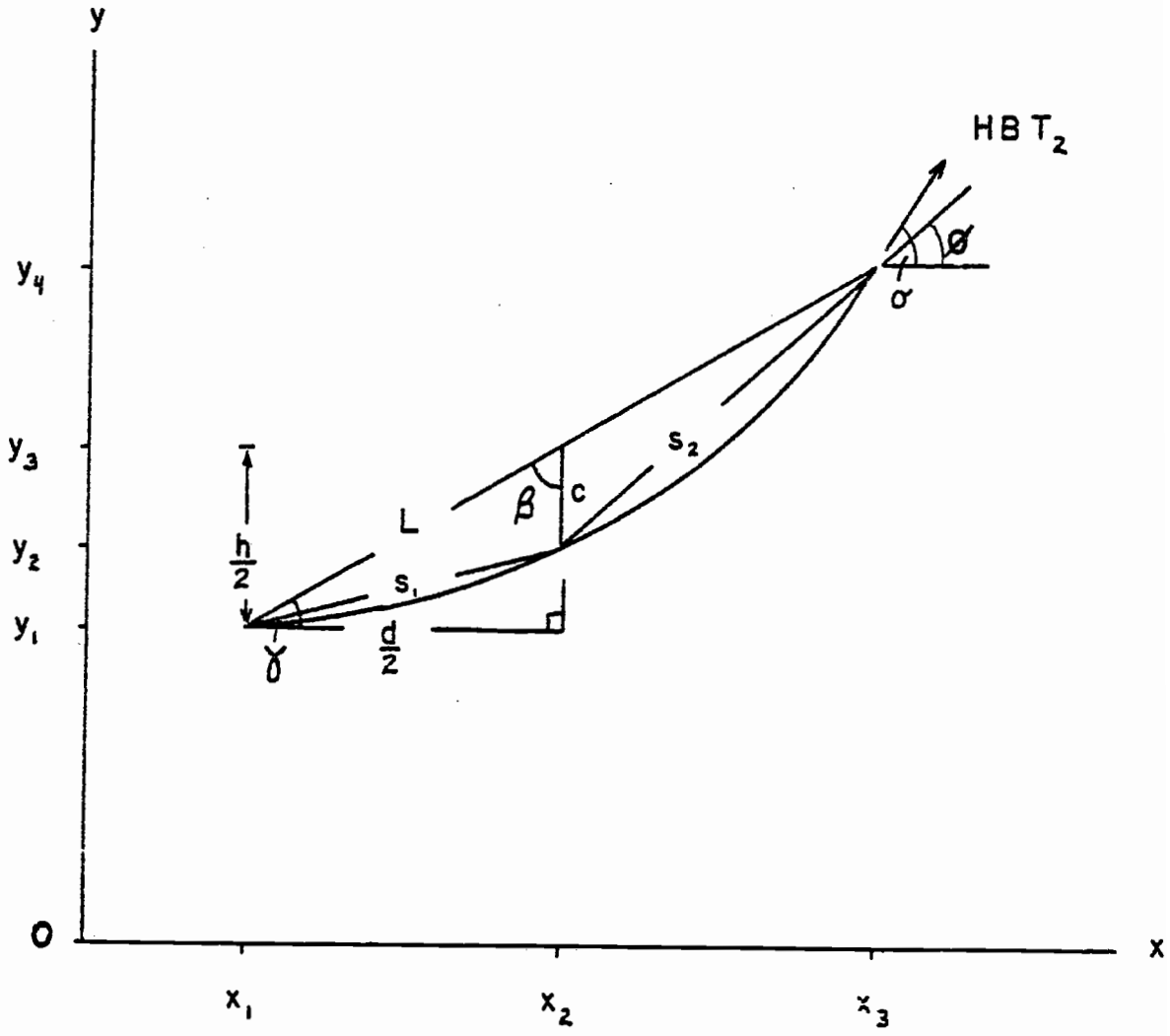

Figure 11. Haulback Cable Segment

In the figure above,

$$c = .01\ d \qquad \text{eq. 29}$$

where .01 is the decimal deflection, and

$$L = (h^2 + d^2)^{\frac{1}{2}}/2. \qquad \text{eq. 30}$$

The angles in the triangle are

$$\gamma = \tan^{-1} h/d \qquad \text{eq. 31}$$

and

$$\beta = \tan^{-1} d/h\ . \qquad \text{eq. 32}$$

Using the Cosine Law,

$$s_1 = (L^2 + c^2 - 2Lc \cos \beta)^{\frac{1}{2}} \qquad \text{eq. 33}$$

and

$$s_2 = (L^2 + c^2 - 2Lc \cos (180 - \beta))^{\frac{1}{2}} \quad . \qquad \text{eq. 34}$$

Adding these two segment together gives an initial approximation for HB s, the length of the haulback. The approximate direction, angle ϕ, at which HB T_2 acts is found by using the Law of Sines:

$$\phi = 90 - \sin^{-1}\left[\frac{L}{s_2} \sin (180 - \beta)\right] \quad . \qquad \text{eq. 35}$$

The next step is to solve for an approximate value of m using catenary equations. Carson (1977) describes an algebraic solution for m in terms of h, s, and σ.

Equation 13 is rearranged into the form

$$\sinh (d/2m) = ((s^2-h^2)/4m^2)^{\frac{1}{2}}$$

or

$$d/2m = \sinh^{-1} ((s^2-h^2)/4m^2)^{\frac{1}{2}} \quad . \qquad \text{eq. 36}$$

Using the hyperbolic function identity

$$\sinh^{-1} (x) = \coth^{-1} (1 + x^2)^{\frac{1}{2}}/x$$

and substituting, results in the form

$$d/2m = \coth^{-1} (1 + (s^2-h^2)/4m^2)^{\frac{1}{2}}/((s^2-h^2)/4m^2)^{\frac{1}{2}}$$

which simplifies to

$$\coth (d/2m) = (4m^2/(s^2-h^2) + 1)^{\frac{1}{2}} \quad . \qquad \text{eq. 37}$$

This equation is then substituted into equations 7 and 8.

$$T_2 = (w/2) (s (4m^2/(s^2-h^2) + 1)^{\frac{1}{2}} + h) \qquad \text{eq. 38}$$

and

$$V_2 = (w/2)\ \ h\ (4m^2/(s^2-h^2) + 1)^{\frac{1}{2}} + s) \quad . \qquad \text{eq. 39}$$

These equations can describe the angle σ in the form

$$\sin \sigma = \frac{V_2}{T_2} = \frac{h(4m^2/(s^2-h^2)+1)^{\frac{1}{2}} + s}{s(4m^2/(s^2-h^2)+1)^{\frac{1}{2}} + h}$$

which can be simplified to

$$s \sin \sigma\ (4m^2/(s^2-h^2) + 1)^{\frac{1}{2}} + h \sin \sigma = h\ (4m^2/(s^2-h^2) + 1)^{\frac{1}{2}} + s$$

$$(s \sin \sigma - h)(4m^2/(s^2-h^2) + 1)^{\frac{1}{2}} = s - h \sin \sigma$$

$$4m^2/(s^2-h^2) + 1 = \left[\frac{s - h \sin \sigma}{s \sin \sigma - h}\right]^2 - 1$$

$$4m^2 = (s^2-h^2)\left[\frac{s-h \sin\sigma}{s \sin \sigma-h}\right]^2 - 1$$

and finally

$$m = \frac{1}{2}\left[(s^2 - h^2)\left[\left[\frac{s-h \sin \sigma}{s \sin \sigma-h}\right]^2 - 1\right]\right]^{\frac{1}{2}} \quad . \qquad \text{eq. 40}$$

An initial value for m can be determined by substituting the angle ϕ for σ. The tensions and coordinates of the haulback can be calculated using the following equations:

$$\text{HB } s = (h^2 + (2m \sinh (d/2m))^2)^{\frac{1}{2}} \qquad \text{eq. 13a}$$

$$\text{HB } T_2 = (w/2)\ (s \coth (d/2m) + h) \qquad \text{eq. 7a}$$

$$y_4 = \text{HB } T_2/w \qquad \text{eq. 15a}$$

$$y_1 = y_4 - h \qquad \text{eq. 40}$$

$$X_3 = m \cosh^{-1} (y_4/m) \qquad \text{eq. 16a}$$

$$X_2 = X_3 - (d/2) \qquad \text{eq. 41}$$

$$X_1 = X_3 - d \qquad \text{eq. 42}$$

$$Y_2 = m \cosh (X_2/m) \qquad \text{eq. 14a}$$

$$Y_3 = Y_1 + h/2 \qquad \text{eq. 43}$$

$$c' = Y_3 - Y_2 \qquad \text{eq. 44}$$

Equation 43 calculates the vertical distance at midspan between the chord slope and the cable segment based on this approximate value of m. The iterative algorithm now compares c' to the original distance c. If the distances do not agree within an allowable tolerance set at .01 feet, a new approximation for m is made using

$$m_{new} = (c'/c)\, m_{old} \quad . \qquad \text{eq. 45}$$

The algorithm now returns to equation 11a and repeats this sequence until the deflections agree. This algorithm also converges on the answer rapidly and usually doesn't require more than two or three iterations. Tension HB H and HB V_1 identified in static equilibrium equations 17 and 18 are solved as follows:

$$\text{HB H} = m\, w \qquad \text{eq. 6a}$$

$$\text{HB } T_1 = y_1\, w \qquad \text{eq. 15a}$$

$$\text{HB } V_1 = (\text{HB } T_1^2 - \text{HB } H^2)^{\frac{1}{2}} \qquad \text{eq. 46}$$

The remaining unknowns in equations 17 and 18 are the tensions for the mainline and skyline. The solution for these tensions also requires an iterative algorithm. Again the start of the iteration begins with an approximation for the catenary parameter of the cable segment, in this case the skyline. The starting point is based on an approximation that SL H = Wg which gives the initial value of

$$\text{SL } m = \text{SL } H/w \quad . \qquad \text{eq. 6b}$$

Based on this value of m, the skyline length and tensions are calculated according to the following equations:

$$SL\ s = (h^2 + (2m \sinh (d/2m))^2)^{\frac{1}{2}} \qquad \text{eq. 13b}$$

$$SL\ T_1 = (w/2)\ (s \coth (d/2m) - h) \qquad \text{eq. 9b}$$

$$SL\ V_1 = (w/2)\ (h \coth (d/2m) - s) \qquad \text{eq. 11b}$$

$$SL\ H = m\ w \qquad \text{eq. 6b}$$

Static equilibrium equation 17 is used to solve for ML H according to

$$ML\ H = SL\ H - SL\ T_1 \cos 0 + HB\ H \ . \qquad \text{eq. 17}$$

This leads to the calculation of the mainline catenary parameter

$$ML\ m = ML\ H/w \ . \qquad \text{eq. 6c}$$

The mainline length and tensions are calculated as follows:

$$ML\ s = (h^2 + (2m \sinh (d/2m))^2)^{\frac{1}{2}} \qquad \text{eq. 13c}$$

$$ML\ T_2 = (w/2)\ (s \coth (d/2m) + h) \qquad \text{eq. 7c}$$

$$ML\ V_2 = (w/2)\ (h \coth (d/2m) + s) \ . \qquad \text{eq. 8c}$$

Static equilibrium equation 18 is used to solve for Wg', the gross weight estimate based on the approximation of m, the skyline catenary parameter.

$$Wg' = SL\ T_1 \sin \theta + SL\ V_1 + HB\ V_1 - ML\ V_2 \qquad \text{eq. 18}$$

If the Wg' does not agree with the correct weight Wg within an allowable tolerance set at .01 lbs, the iterative algorithm calculates a new approximation for the skyline m using

$$m_{new} = (Wg/Wg')\ m_{old} \ . \qquad \text{eq. 47}$$

The algorithm then returns to equation 13b and repeats this

sequence until the gross weights agree. When agreement is reached, the calculation of the skyline, mainline and haulback forces is completed. The flow chart of a computer program written for the Hewlett Packard (HP) 41-C displays the iterative algorithm and is shown in Figure 12. The program steps for the HP 41-C are listed in Appendix 2.

Critical Run Results

Table 3 lists the critical run theoretical values for the angle θ of the skyline segment. The calculation of these values was based on the maximum mainline design tension for the Christy yarder and the dimensions d and h measured during the field tests. The design tension for the Christy yarder was limited to 11,200 lbs the safe working load of a 9/16" cable. The rated mid-drum pull for the Christy yarder is 20,000 lbs. Table 3 also lists the critical run values measured during the field tests. These values are less than those calculated because the amount of mainline tension applied by the yarder did not come close to the design tension.

Table 3.

A Comparison Between the Theoretical and Measured Values for the Critical Run Angle θ of the Skyline Segment

Test	Theoretical angle°	Measured angle°
A	66.3	52.6
B	64.4	51.2
C	63.6	51.8

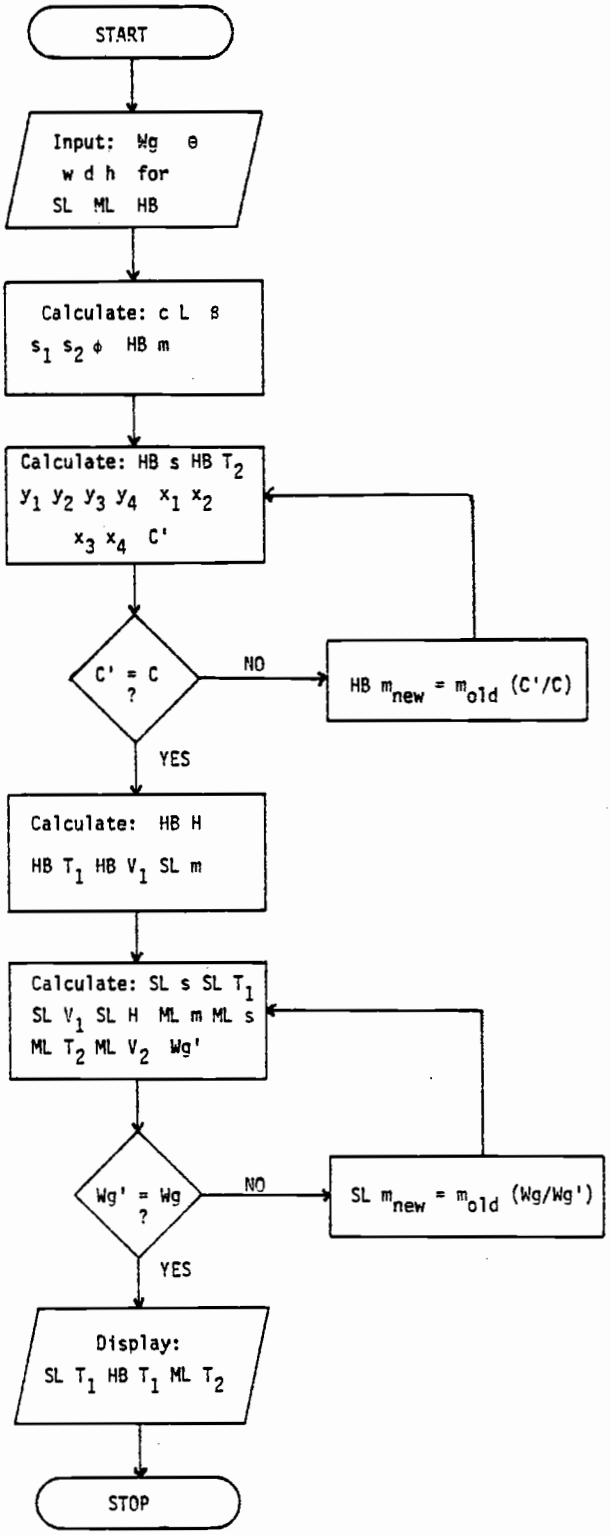

Figure 12. Computer Program Flowchart.

Table 4 lists the calculated and measured static cable tensions for the skyline, mainline and haulback when the carriage is positioned just prior to passage of the support jack for the critical runs. The calculated tensions are based on a θ of 52 degrees, a Wg of 1,100 lbs and a haulback deflection of one percent.

Table 4.

Comparison of Calculated and Measured Static Cable Tensions for Critical Runs

	SL (lbs)		ML (lbs)		HB (lbs)	
Test	Calc.	Meas.	Calc.	Meas.	Calc.	Meas.
A	1654	1745 (± 15)	1718	1660 (± 15)	961	935 (± 15)
B	1969	2005 (± 15)	1883	1920 (± 15)	936	985 (± 15)
C	2471	2480 (± 15)	2130	2175 (± 15)	922	910 (± 15)

Values in parentheses denote the range of measurement error.

CHAPTER VII

DISCUSSION

The static cable tensions listed on Table 4 allow a comparison between the calculated and measured values. All of the calculated tensions are reasonably close to the range of the measured tensions; they did not vary from the measured tensions by more than 5 percent.

A comparison between the measured static tensions and the dynamic tensions displayed in Figure 9 shows higher static tensions when the carriage is about to pass the support jack. The differences between the static and dynamic tensions could be related to the difficulty of operating the yarder consistently for both the static and dynamic tests. In addition, there are inherent differences in the analysis of static and dynamic forces. An imbalance of forces in the direction that the loaded carriage needs to travel is a requirement for movement along the skyline. A static analysis does not consider the positive effect of loaded carriage momentum on carriage passage.

The recordings of the dynamic tensions show that the skyline tension decreased as the carriage passed from the upper span to the support jack. The tension reached its lowest value just as the carriage passed onto the support jack.

Fodge's (1981) analysis of the maximum loading on the intermediate support cable included: the forces due to the weight of

the loaded carriage, the skyline forces acting on the support jack when the tension was at or near the skyline pretension, and the forces of the cables attached to the carriage. His analysis was derived for the uphill yarding configuration which did not have a haulback attached to the carriage.

This low point in the dynamic skyline tension therefore represents the skyline pretension described in Fodge's analysis. As the carriage passes over the support jack, the weight of the carriage and force component ML V_2 are supported for a moment entirely by the support jack and intermediate support line rather than the skyline. Skyline pretension is the unloaded skyline tension and is directly related to skyline length or equivalently skyline deflection. The skyline pretensions decreased as the skyline deflection was increased for each run in a given test. There does not appear to be any significant difference between the skyline pretensions for the critical runs in the three tests.

The mainline and haulback dynamic tensions increased as the carriage approached the support jack. For the runs in a given test, these tensions increased as the skyline deflection increased. A greater mainline tension, which in turn increased the haulback tension, was required to advance the carriage over the support jack as the skyline length increased. The mainline and haulback tensions recorded as the carriage passed the support jack during a critical run, were greatest for test C, which had the greatest percent change in span chord slopes.

All of the dynamic recordings showed fluctuations in cable tensions as the carriage surged off of the support jack. The skyline tension increased to its highest value immediately after the carriage left the support jack and fluctuated until the carriage proceeded further into the lower span. The mainline and haulback tensions peaked and fluctuated as the carriage surge pulled the haulback taut. It was found that maintaining a taut, or higher tension, haulback during the carriage passage portion of the yarding cycle helped reduce these fluctuations.

The static cable tensions displayed on Figure 8 show an increase in mainline and haulback tensions while skyline tensions decreased as the skyline deflection was increased for successive runs in a given test. A comparison of the static tensions measured for the critical runs in the three tests shows that the mainline and skyline tensions increase as the percent change in span chord slopes increases. As the change in span chord slope increases, the direction of the mainline tension acting at the carriage becomes less aligned with the direction that the carriage has to travel over the skyline. Consequently, the magnitude of the mainline tension has to become greater to contribute a force component great enough to maintain the static position where the carriage is about to advance onto the support jack.

One key to the solution of the static analysis development was the determination of the angle θ, the slope of the skyline segment between the support jack and the carriage. During the field tests

this angle reached approximately 52 degrees as the skyline deflection was increased and the critical run was achieved.

Table 3 compares the theoretical and measured values for θ. The calculation of the theoretical θ was based on the maximum design tension for the mainline. During the field tests the yarder was operated in a conservative manner and the measured mainline tensions were well below the design tension. Consequently, the angle θ measured for the critical runs were less than the theoretical values. Figure 13 shows the carriage as it approaches the support jack during a critical run.

Figure 13. The Carriage Approaching the Support Jack During a Critical Run.

Brantigan tested the uphill multi-span yarding configuration and found that this angle θ approached 90 degrees for the critical run. During the field tests in this study the loaded carriage was yarded up and over the support jack in a manner similar to the uphill configuration. The haulback was used as a mainline to pull the carriage along the skyline, while the actual mainline was allowed to go slack. As the skyline length was increased for the beginning of the test runs it became more difficult to pull the carriage over the support jack. Eventually the skyline length became too long to allow the carriage to pass uphill, and indeed the slope of the skyline segment between the carriage and the support jack was nearly vertical. However, the skyline lengths which prohibited the loaded carriage from passing uphill over the support jack were shorter than the lengths which prohibited downhill carriage passage. The skyline lengths which prohibited uphill carriage passage were reached before the test runs for downhill yarding were started.

The difference in the skyline length for the uphill and downhill yarding configuration which prohibits carriage passage, can be explained by examining the effect of the skyline segment between the carriage and the tail tree. As the carriage approaches the support jack, the skyline segments form a resultant force, the direction of which is a function of the slope of the span and the skyline length. For a given skyline length and chord slope arrangement, the skyline resultant in the downhill configuration contributes more force in the direction that the carriage needs to travel. The skyline segment

between the carriage and the tail tree drops away from the carriage in the uphill configuration and contributes less lift as the skyline length is increased.

Figures 8a, b and c show the relationship between carriage passage difficulty for downhill yarding and upper span skyline deflection. It is not surprising that the difficulty in passing the support jack increases as skyline deflection increases.

Figure 14 displays the upper span skyline deflection for the critical runs versus the percent change of span chord slopes for the tests. This figure shows the relationship between successful carriage passage, upper span skyline deflection, and the percent change in span chord slopes. As the percent change in span chord slopes increased, the skyline deflection at which the critical run was achieved, decreased.

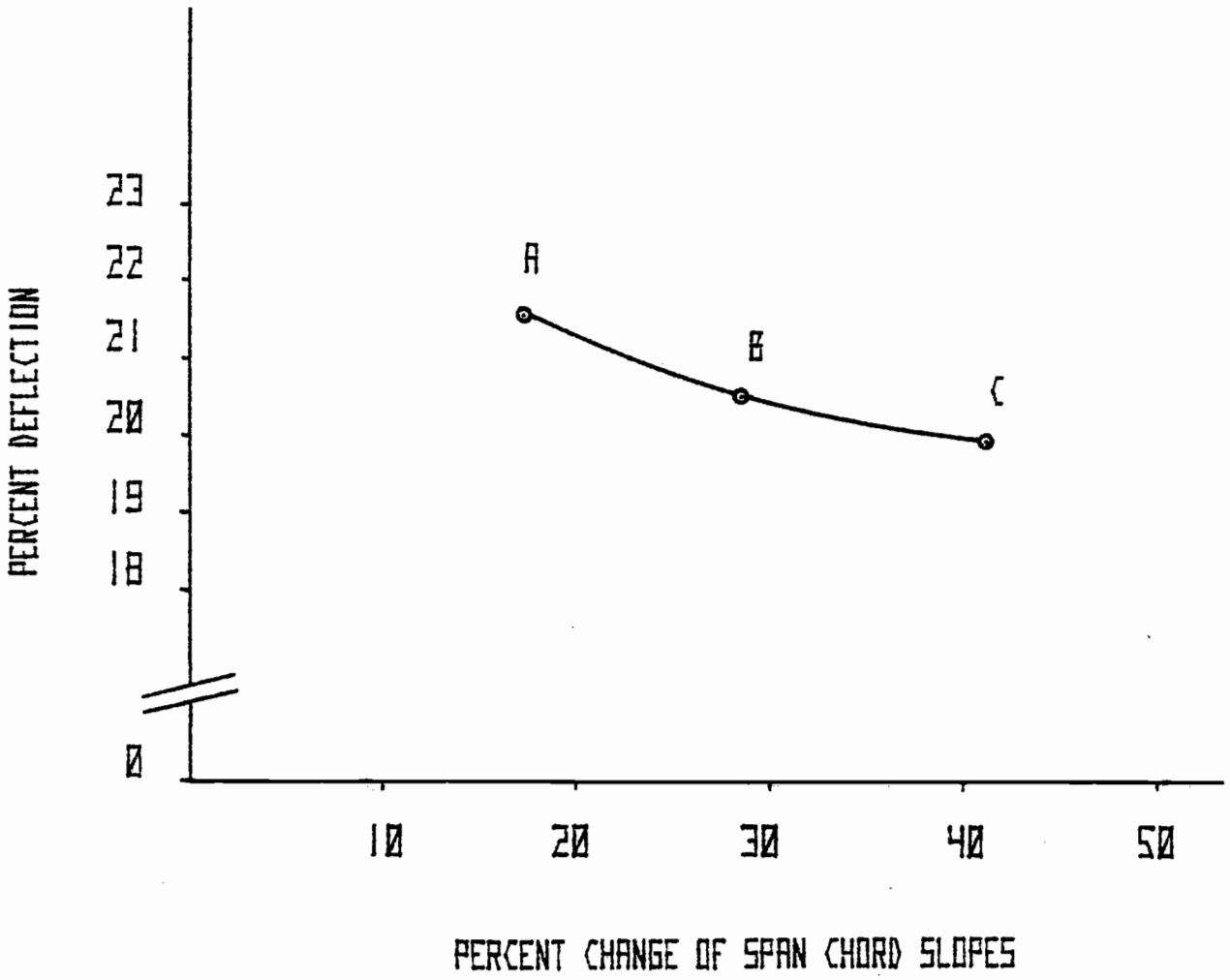

FIGURE 14. UPPER SPAN SKYLINE DEFLECTION FOR CRITICAL RUNS VS. PERCENT CHANGE OF SPAN CHORD SLOPES FOR TESTS A B & C.

CHAPTER VIII

CONCLUSIONS AND RECOMMENDATIONS FOR FUTURE RESEARCH

This study determined the relationship between upper span skyline deflection, the percent change in span chord slopes, and their influence on successful carriage passage during downhill yarding. A catenary analysis of the static cable tensions was presented.

The catenary analysis of cable tensions was based on the observation that maintaining a taut haulback during carriage passage prevents the carriage from surging uncontrolled off of the support jack. Maintaining a taut haulback reduced the fluctuations of dynamic cable tensions.

The results of the field tests showed that as the change in the span chord slopes increases, the skyline deflection at which carriage passage becomes difficult, decreases. A logging engineer should be aware of the implications when increasing skyling deflection to increase payload capability for downhill yarding on difficult convex slopes. A loaded carriage has increasing difficulty in passing a support jack as skyline deflection becomes excessive.

The question of how much skyline deflection will prohibit carriage passage has not been answered in this paper. The data displayed on Figure 14 is not intended to be used as a general guideline for determining conditions at which an unsuccessful

carriage passage will occur. The magnitude of the skyline deflections for the critical runs are in part a function of the relatively light gross load used for the field tests. The results of this study are specific to these tests conducted with one gross load, one combination of cable sizes and one support jack and carriage combination.

However, it is not likely that loggers will operate with skyline deflections great enough to impede carriage passage. Skyline deflection is limited by the clearance required along the profile between the skyline and ground for carriage and choker length.

During the field testing, it was also observed that yarding the loaded carriage uphill over the support jack became impossible as skyline deflections were increased to levels which still allowed successful carriage passage for downhill yarding.

Suggestions for future research include determine the relationship between successful carriage passage, gross load and skyline deflection. In addition, determining the relationship between skyline slippage over the support jack shoe and skyline deflection during carriage passage would allow a more complete analysis of cable forces.

List of References

1. Binkley, Virgil W. and John Sessions. 1978. Chain and Board Handbook for Skyline Tension and Deflection. U.S.D.A. Forest Service, Volume II Logging Systems Library. pp. 193.

2. Brantigan, Richard T. 1978. Critical Conditions for Carriage Passage at the Support Jack for Uphill Yarding. A Thesis. Oregon State University, Corvallis, Oregon. pp. 111.

3. Carson, Ward W. 1977. Analysis of a Single Cable Segment: Forest Science, Vol. 23 (2): 238-252.

4. Fodge, Francis W. 1981. Engineering Analysis of Forces Created in Two Tree Intermediate Supports During Multi-Span Logging. Master of Forestry Paper. School of Forestry, Oregon State University, Corvallis, Oregon. pp. 69.

5. McGonagill, Keith L. 1977. Logging Systems Guide. U.S.D.A. Forest Service, Alaska Region, Division of Timber Management, Juneau, Alaska, Series No. R10-21.

6. Merriam, J.L. 1978. Engineering Mechanics Volume 1 Statics. John Wiley and Sons, Inc. New York. pp. 398.

7. Peters, Penn A. and D. E. Aulerich. 1977. Timber Harvest using an Intermediate Support System. American Society of Agricultural Engineers, Paper 77-1564. pp. 11.

APPENDICES

APPENDIX 1

Equipment Specifications

Cristy Small Wood Yarder

31 ft. 12" x 12" steel spar, hydraulically raises

105 HP 3-53 GMC diesel engine

AT 540 4-speed Allison automatic transmission

22" diameter x 4" wide band brakes

15" diameter x 3½" (shoe type) drive clutches

Mainline drum capacity - 1,100 ft. 9/16" line

mid-drum line speed - 1,300 ft./min

mid-drum line pull - 20,000 lbs.

Skyline drum capacity - 1,200 ft 5/8" line

mid-drum line speed - 1,100 ft./min

mid-drum line pull - 22,000 lbs.

Haulback capacity - 2,400 ft. 7/16" line

3 guyline drums - 210 ft. 9/16" line

1 snap guy - 190 ft. 9/16" line

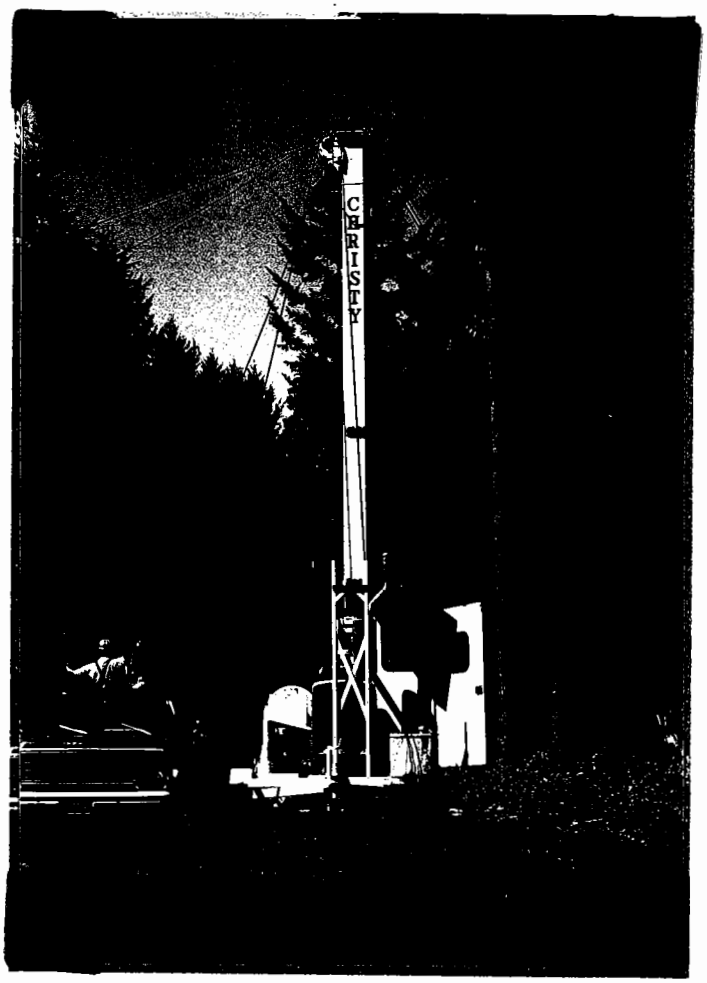

Load Cells

The load cells used for this study were constructed by the Forest Engineering Dept. of OSU. Each load cell is comprised of a high tensile strength steel bar with strain gage resistors mounted on the horizontal and vertical faces machined along the central axis.

Validyne Model SG71 Strain Gage Amplifier

Output Voltage:	± 10 V DC
Input Sensitivity for 10 VDC Output:	1, 2.5, 5, 10, 25 or 50 m V/V switch options
Bridge Excitation:	5 V DC, 50 mA maximum
Power Input:	± 15 V DC (supplied from MC1 module case)

Validyne Model MC1 - 10/20 Channel Module Case

Power Input:	117/234 V AC, 50-400 Hz (powered by a 12 V DC car battery coupled with an inverter to supply 110 V AC during field tests)
Power Output:	± 15 V DC, tracking 60 watts

Validyne Model PM212 Digital Panel Meter

Power Input:	± 15 V DC @ 35 mA from MC1 chassis
Stability (drift):	± 1 digit of input
Accuracy-normal:	.25% of full scale

Brush (Gould) Model 222 (battery) Strip Chart Recorder

Frequency response:	DC - 30 Hz @ ± 2% of f.s.
Input Sensitivity:	1 mV/div. to 500 V f.s.
Chart speeds:	1, 2, 5, 10, 25 and 50 mm/sec

APPENDIX 2

HP 41-C Computer Program Listing

```
01♦LBL "MULTI"
02 "UPPER SL D=?"
03 PROMPT
04 STO 00
05 "UPPER SL H=?"
06 PROMPT
07 STO 01
08 "SL WT=?"
09 PROMPT
10 STO 02
11 "LOWER ML D=?"
12 PROMPT
13 STO 03
14 "LOWER ML H=?"
15 PROMPT
16 STO 04
17 "ML WT=?"
18 PROMPT
19 STO 05
20 "UPPER HB D=?"
21 PROMPT
22 STO 06
23 "UPPER HB H=?"
24 PROMPT
25 STO 07
26 "HB WT=?"
27 PROMPT
28 STO 08
29 "GROSS WT=?"
30 PROMPT
31 STO 09
32 RCL 06
33 .01
34 *
35 STO 10
36 RCL 06
37 RCL 07
38 R-P
39 2
40 /
41 STO 11
42 RCL 06
43 RCL 07
44 /
45 ATAN
46 STO 12
47 RCL 11
48 X↑2
49 RCL 10
50 X↑2
51 +
52 RCL 12
53 COS
54 RCL 10
55 *
56 RCL 11
57 *
58 2
59 *
60 -
61 SQRT
62 RCL 11
63 X↑2
64 RCL 10
65 X↑2
66 +
67 180
68 RCL 12
69 -
70 COS
71 RCL 10
72 *
73 RCL 11
74 *
75 2
76 *
77 -
78 SQRT
79 STO 13
80 +
81 STO 14
82 180
83 RCL 12
84 -
85 SIN
86 RCL 11
87 *
88 RCL 13
89 /
90 ASIN
91 90
92 X<>Y
93 -
94 STO 15
95 RCL 14
96 RCL 15
97 SIN
98 RCL 07
99 *
100 -
```

```
101 RCL 14
102 RCL 15
103 SIN
104 *
105 RCL 07
106 -
107 /
108 X↑2
109 1
110 -
111 RCL 14
112 X↑2
113 RCL 07
114 X↑2
115 -
116 *
117 SQRT
118 2
119 /
120♦LBL 01
121 STO 16
122 2
123 *
124 RCL 06
125 X<>Y
126 /
127 STO 17
128 XEQ 04
129 RCL 16
130 *
131 2
132 *
133 X↑2
134 RCL 07
135 X↑2
136 +
137 SQRT
138 STO 18
139 RCL 17
140 XEQ 05
141 *
142 RCL 07
143 +
144 RCL 08
145 *
146 2
147 /
148 STO 19
149 RCL 08
150 /
151 STO 22
152 RCL 07
153 -
154 STO 21
155 RCL 22
156 RCL 16
157 /
158 STO 31
159 X↑2
160 1
161 -
162 SQRT
163 RCL 31
164 +
165 LN
166 RCL 16
167 *
168 STO 23
169 RCL 06
170 -
171 STO 24
172 RCL 06
173 2
174 /
175 +
176 STO 25
177 RCL 16
178 /
179 E↑X
180 LASTX
181 CHS
182 E↑X
183 +
184 2
185 /
186 RCL 16
187 *
188 STO 26
189 RCL 21
190 RCL 07
191 2
192 /
193 +
194 RCL 26
195 -
196 STO 27
197 RCL 10
198 -
199 ABS
200 .01
```

```
201 X>Y?
202 GTO 02
203 RCL 27
204 RCL 10
205 /
206 RCL 16
207 *
208 GTO 01
209*LBL 02
210 SF 01
211 RCL 21
212 RCL 08
213 *
214 STO 20
215 RCL 16
216 RCL 08
217 *
218 STO 28
219 RCL 20
220 X↑2
221 RCL 28
222 X↑2
223 -
224 SQRT
225 STO 29
226 GTO 03
227*LBL 04
228 E↑X
229 LASTX
230 CHS
231 E↑X
232 -
233 2
234 /
235 RTN
236*LBL 05
237 STO 30
238 E↑X
239 RCL 30
240 CHS
241 E↑X
242 +
243 RCL 30
244 E↑X
245 RCL 30
246 CHS
247 E↑X
248 -
249 /
250 RTN
251*LBL 03
252 RCL 09
253 RCL 02
254 /
255*LBL 06
256 STO 32
257 2
258 *
259 RCL 00
260 X<>Y
261 /
262 STO 33
263 XEQ 04
264 RCL 32
265 *
266 2
267 *
268 X↑2
269 RCL 01
270 X↑2
271 +
272 SQRT
273 STO 34
274 RCL 33
275 XEQ 05
276 STO 35
277 *
278 RCL 01
279 -
280 RCL 02
281 *
282 2
283 /
284 STO 36
285 RCL 35
286 RCL 01
287 *
288 RCL 34
289 -
290 RCL 02
291 *
292 2
293 /
294 STO 37
295 RCL 32
296 RCL 02
297 *
298 STO 38
299 RCL 36
300 52
```

```
301 COS
302 *
303 -
304 RCL 28
305 +
306 RCL 05
307 /
308 2
309 *
310 STO 39
311 RCL 03
312 X<>Y
313 /
314 XEQ 04
315 RCL 39
316 *
317 X↑2
318 RCL 04
319 X↑2
320 +
321 SQRT
322 STO 40
323 RCL 03
324 RCL 39
325 /
326 XEQ 05
327 STO 41
328 RCL 40
329 *
330 RCL 04
331 +
332 RCL 05
333 *
334 2
335 /
336 STO 42
337 RCL 41
338 RCL 04
339 *
340 RCL 40
341 +
342 RCL 05
343 *
344 2
345 /
346 CHS
347 RCL 29
348 +
349 RCL 37
350 +
351 RCL 36
352 52
353 SIN
354 *
355 +
356 STO 43
357 VIEW 43
358 RCL 09
359 -
360 ABS
361 .01
362 X>Y?
363 GTO 07
364 RCL 32
365 RCL 09
366 RCL 43
367 /
368 *
369 GTO 06
370*LBL 07
371 CF 01
372 TONE 5
373 "SL="
374 ARCL 36
375 AVIEW
376 STOP
377 "ML="
378 ARCL 42
379 AVIEW
380 STOP
381 "HB="
382 ARCL 20
383 AVIEW
384 STOP
385 END
```